478 Received 1/16/76

Proposal to Search for Intermediate Boson Production in Proton Proton Collisions at 200 GeV in the Center of Mass

R. Huson, P. Livdahl, R. Stiening,
L. Teng, F. Turkot, and J. K. Walker* (F.N.A.L.)

*Spokesman.

I. Introduction

II. Physics Discussion

III. Characteristics of the Small Storage Ring

1. Choice of Location
2. Geometry and Lattice
3. Long Straight Sections
4. Beam Characteristics and Magnet Aperture
5. Extraction from Ming Ring
6. Injection and Stacking
7. Vacuum and Mode of Operation
8. Luminosity and Tune Shift

IV. Detection Apparatus

1. Kinematics
2. General Characteristics
3. Detector Concept
4. Detector Detail
5. Calibration of Detector
6. Detector Development

V. Trigger and Event Rates

1. Trigger
2. Event Rate for $W^{\pm}$ Detection
3. Other Reactions
4. Backgrounds

VI. Cost Estimate and Schedule

VII. Future Developments

VIII. Conclusions

Appendix 1. Tunnel and Experimental Hall Conventional Construction.
Appendix 2. Design of the Ring Magnets.
Appendix 3. High Vacuum System.
Appendix 4. Detection System Costs.
Appendix 5. Other Experimental Options for Achieving 200 GeV in the C.M.S.
Appendix 6. Miscellaneous.

I. Introduction

Renormalizable gauge models of weak and electromagnetic interactions require the existence of charged intermediate vector bosons $W^{\pm}$, heavy leptons or neutral vector bosons Z^{o} (or both), and at least one neutral scalar: the "Higgs particle" ϕ^{o}. Although the original model of Weinberg and Salam is so constructed that $M_W \geq$ 37 GeV and $M_Z \geq 74$ GeV, other reasonable models exist in which these vector boson masses can be considerably smaller. It appears very likely that these or other entirely new particles may be discovered in the mass range 20 to 100 GeV.

The most direct way of testing the underlying theory of weak interactions is to search for the intermediate vector bosons $W^{\pm}$ and Z^{o}. We propose performing this search by constructing a small high current ($\sim$ 1 Amp) storage ring which will allow us to study collisions between 25 GeV protons and the normal accelerating proton beam in the main ring of the Fermilab 400 GeV synchrotron. There will be no disruption of the standard Fermilab experimental program involving experiments with internal target and external beams. In the first phase of the experiment a peak energy of 200 GeV in the center of mass system will be achieved with a luminosity of 10^{31} cm^{-2} sec^{-1}. The total cross section for $W^{\pm}$ production, where $M_W \ll 200$ GeV, is expected to be $\gtrsim 10^{-33}$ cm^{2}. Thus, good production rates of $W^{\pm}$ are expected over a large range of mass.

The proposed detector, with close to 4π solid angle, permits identification and momentum analysis of muons of both charge from the reactions

$$p + p \rightarrow W^{\pm} + \text{Anything}$$
$$\hookrightarrow \mu^{\pm} + \text{Anything}$$
$$p + p \rightarrow Z^{o} + \text{Anything}$$
$$\hookrightarrow \mu^{+} + \mu^{-}$$

In addition, the detector provides a rough measurement of the energy and momentum of the hadronic cascades by the calorimetric technique.

Two characteristics of the events will be used to identify the production of W mesons. These are the observation of a peak in the cross section for muon production at $p_{\perp} \simeq M_W/2$, and observation of a large imbalance of transverse momentum corresponding to a missing neutrino. Backgrounds from the continuum of $\mu^+\mu^-$ pairs and known sources of single muons should be small.

The neutral intermediate boson Z^o probably has a smaller cross section than its charged counterpart. Its production will be signalled by the observation of a resonant peak in the $\mu^+\mu^-$ mass spectrum.

An estimate for construction of the tunnel, storage ring, and detection apparatus results in a total cost of less than four million dollars. Apart from the conventional construction cost of \$1 M, approximately \$1.5 M would be required per year for two years to mount this experiment.

A second phase of the experiment would involve raising the cms energy to 400 GeV and increasing the luminosity up to 10^{32} cm^{-2} sec^{-1}.

II. Physics Discussion

Recent dramatic theoretical developments in our understanding of renormalizable gauge models of weak and electromagnetic inter-

actions have been given impetus with the experimental confirmation of the existence of neutral weak currents. All of the varieties of these models require the existence of charged and neutral intermediate vector bosons $W^{\pm}$, Z^{o}. The parton model predicts a copious production of these bosons in high energy proton proton collisions. Partons in one proton annihilate with antipartons in the other proton to produce a massive boson by virtue of their large opposite momenta. The resulting cross section is point-like and obeys a scaling law characteristic of parton models. The same arguments were first applied to the electromagnetic process

$$p + p \rightarrow \mu^{+} + \mu^{-} + \text{anything}.$$

The model predicts large cross sections in this case also (even at large $M^2_{\mu^+\mu^-}/s$) and a similar cross section scaling law. Recent predictions[1] of the parton model using parton and anti-parton distributions derived from deep inelastic electron scattering appear to describe available neutrino inelastic scattering data and in addition, all available data of electromagnetic production of lepton pairs in proton proton collisions. The latter are the BNL data on production of μ and e pairs and the Fermilab data on production of μ pairs.

The production of $W^{\pm}$ is related by the conserved vector current hypothesis to the production of e^+e^- or $\mu^+\mu^-$ pairs of the same mass at the same center-of-mass energy. However, CVC does not say anything about the semi-weak axial current, nor does it relate the semi-weak current to the isoscalar electromagnetic current. Hence the assumption of CVC and the parton model as described above provides a lower bound for the production of W's. With these assumptions we obtain

$$\sigma_W \gtrsim 0.09\ M_W^3\ \left(\frac{d\sigma}{dM_W}\right)_{\mu^+\mu^-}$$

where $\frac{d\sigma}{dM_W}$ is the cross section for the electromagnetic production of a lepton pair of mass M_W and

$$\frac{d\sigma}{dM_W} = \frac{8\pi\alpha^2}{3Q^3} \int_0^1 dx_1 \int_0^1 dx_2\ \delta(x_1x_2-Q^2/s)\,[x_1x_2G(x_1,x_2)]$$

$$\begin{aligned} \text{with } G(x_1,x_2) = & \frac{4}{9}\,[u(x_1)\ \bar{u}(x_2) + \bar{u}(x_1)\ u(x_2)] \\ & + \frac{1}{9}\,[d(x_1)\ \bar{d}(x_2) + \bar{d}(x_1)\ d(x_2)] \\ & + \frac{1}{9}\,[s(x_1)\ \bar{s}(x_2) + \bar{s}(x_1)\ s(x_2)]. \end{aligned}$$

The parton and anti-parton distribution functions are choosen to be the so called modified Kuti-Weisskopf functions with constants determined from the deep inelastic electron scattering data. Figure 1 shows the expectations of the production cross section for lepton pairs together with the available data. The agreement is sufficiently good that it gives some confidence in extrapolating the predictions to 200 GeV in the center-of-mass. Figure 2 shows the predicted lower bound of the total cross section for production of $W^{\pm}$ mesons of various mass as a function of the main ring energy colliding with 25 GeV protons. At 400 GeV main ring energy the cross section has fallen by a little more than a factor of 10 between 40 and 100 GeV W mass.

Production of the $W^{\pm}$ will be detected through the decay

$$W^{\pm} \rightarrow \mu^{\pm} + \nu.$$

The unique signature is a peak in the transverse momentum of the decay muon. At the energy available at the ISR, the cross section

for a mass of 40 GeV compared to 20 GeV has fallen by a factor of 100. It appears possible to study W masses at about one-half the total center of mass energy at either the ISR (30 GeV) or in this proposal (100 GeV). At the peak, the production rate of muons is larger than the non-resonant muons from electromagnetic background by a factor of roughly $1/\alpha$.

The same parton model makes predictions for the cross section for Z^o production. The cross section is somewhat lower than that for the charged W bosons. We shall not discuss Z^o production further as the detector requirements are similar to that for $W^{\pm}$ detection.

Finally, the indications of possible jet like structure in the data of recent ISR experiments should become much more apparent at 200 GeV in the center of mass. It seems likely that jets with transverse momenta up to 20 GeV/c will be observed.

III. Characteristics of the Small Storage Ring

1. Choice of Location

We have chosen to locate the small ring at straight section E of the main ring as shown in Fig. 3. For easy visualization of its size, we mention that it is approximately the size of the booster. Straight section E has been choosen as the location because of its proximity to Butterfield Road which mitigates against its use either in connection with POPAE or future secondary beams. Due to the compact nature of the small ring this location provides ample space for construction and isolation from the public highway. An additional reason for the suitability of this location is the low existing ground level. This minimizes the costs of excavation and tunnel construction. Good load bearing till exists at the tunnel floor elevation. The tunnel size is 7' wide and 7'6" high. More

details of the conventional construction are given in Appendix 1.

2. Ring Geometry and Lattice

The ring is roughly in the shape of a race-track with two semi-circular curved sections ∿ 75 m in radius joined by two straight sections each ∿ 60 m in length. One long straight section (I) runs parallel and next to the MR long straight section in which the 2 beams are brought together to collide with the proper characteristics by dipoles and quadrupoles. The other long straight section (N) is simply bridged across with quadrupoles. The two curved sections are composed of simple FODO cells. The betatron oscillation phase-advance is 90° per cell. The dipoles in one half-cell in the middle of each curved section are omitted to facilitate injection. Figure 4 shows the proposed layout.

The parameters of a normal FODO cell are

Effective total dipole length/half-cell	6.7 m = 2 x 3.35 m
Dipole field	18.06 kG
Bending angle/half-cell	0.13996 rad
Effective quadrupole length	0.5 m
Quadrupole field gradient	± 244.6 kG/m
Equivalent total straight length/half-cell	2.8 m
Cell length	20.0 m
Amplitude function	
β_{max}	34.14 m
β_{min}	5.86 m
Dispersion function	
η_{max}	3.79 m
η_{min}	1.81 m

Phase advance/cell	90°
Equivalent radius of normal cell	71.45 m

One half of a normal cell is shown in Fig. 5.

For the two curved sections (including one straight half-cell in the middle of each curved section) the parameters are:

Number of cells/curved section	$11\frac{1}{2}$ ($\frac{1}{2}$ straight)
Length of a curved section	230 m
Bending angle/curved section	$3.0791 = \pi - 0.0625$
Phase advance/curved section	2.875 (2π)
Total number of cell dipoles	88
Total number of cell quadrupoles	48

The chromaticity of the storage ring must be adjusted by sextupoles located in the short (2 m) straight sections immediately following the quadrupoles. In order not to introduce undesirable harmonics which excite third-integer resonances, the sextupoles should be arranged in groups of 4 located in four consecutive cells. For each transverse plane, we need 16 sextupoles arranged in two troups of 4 in each curved section. The requirements of sextupoles are thus:

Total number of sextupoles	32
Strength of each sextupole ($B''\ell$)	100 kG/m

These sextupoles can also be individually powered to trim out any undesirable harmonics arising from errors in the dipoles and quadrupoles.

Since the storage ring is operated at a fixed energy closed-orbit distortion can be compensated by laterally moving the quadrupoles, and the betatron oscillation tunes can be controlled by adjusting the currents in the F and D quadrupoles.

We also list here the "energy parameters" of the beam.

Kinetic energy	25 GeV
γ	27.64
$B\rho$	864.6 kGm
ρ (at B = 18.06 kG)	47.9 m

3. Long Straight Sections

The neutral long straight section (N) away from the main ring starts and ends on D quadrupoles of the normal cells and is $\sim$ 60 m long. The exact length being dictated by the exact dimensions of the other long straight which, in turn, depends on the rf requirement (see section 6 below). The long straight is matched across by quadrupoles such that the horizontal phase advance is exactly 2π. This will ensure that the horizontal dispersion function is also properly matched. The exact arrangement of the quadrupoles still has to be worked out. But the problem is straightforward and is not expected to give any difficulty. About 8 quadrupoles are needed for matching.

The intersecting long straight section (I) next to the main ring starts and ends on F quadrupoles of the normal cells and contains 6 dipoles to guide the two beams along the orbits shown in Fig. 6. The two beams collide head-on over the central drift space (colliding straight) with a total drift-length of 17.84 m. The three dipoles on either side are mirror reflections and as shown in Fig. 6 are:

<u>Dipole A.</u> This is the first encountered by the beams going away from the colliding straight. It is 1 m long with an 18 kG field and having an aperture of 10 cm (h) x 5 cm (v).

This dipole is used in common by both beams and serves to separate them.

Dipole B. This is a double wide-gap septum dipole with equal and opposite fields in the two gaps. The septum is 5 cm thick. The two gaps have dimensions 50 cm (h) x 5 cm (v) and 20 cm (h) x 5 cm (v) and field intensities ± 12 kG. With a length of 3 m, this dipole produces a bend-angle exactly twice that of dipole A. The orbits of the two beams going through these different gaps are bent in the same direction.

Dipole C. This is identical to dipole A but is used only by the main-ring beam.

Dipoles A, B, C produce a local 3-magnet bump on the main-ring orbit. The maximum inward horizontal orbit deflection in the middle of dipole B varies from 41 cm to 0.91 cm as the main-ring beam is accelerated from 8 GeV to 400 GeV. But, of course, the orbit in the colliding straight remains fixed throughout. The storage-ring orbit is bent by A and B in the same direction with a total angle of 0.0625 rad.

Matching quadrupoles are placed along the storage-ring beam to produce, at the mid-point of the colliding straight

η^* (horizontal and vertical) = 0

β^* (horizontal and vertical) = 4.65 m.

The main ring has a β value at this point of 72 m which is to β^* in the same ratio as the momenta of 400 GeV and 25 GeV. The two beams will then have identical cross-sectional dimensions, at the mid-point.

Based on past experience such a matching section looks possible but the exact arrangement of the matching quadrupoles still has to be worked out. About 12 quadrupoles are needed some of which must be placed between dipole A and B, and hence must have a septum-type design.

The phase advance across long straight I depends on the matching arrangement but should be close to $\sim 2 \times (2\pi)$. Hence the tune of the storage ring will be

$$\nu \sim 2 \times 2.875 \text{ (curved sections)} + 1 \text{ (straight section N)} + 2 \text{ (straight section I)} = 8.75$$

4. Beam Characteristics and Magnet Aperture.

For stacking into the storage ring we use single-turn injection into the booster. The transverse emittance of the beam is, then,

$$\varepsilon = \begin{cases} 0.35\pi \text{ mm-mrad} & @ \ 25 \text{ GeV} \\ 0.0225\pi \text{ mm-mrad} & @ \ 400 \text{ GeV.} \end{cases}$$

At the middle of the colliding straight because of the matched β-values, both the 400 GeV main-ring beam and the 25 GeV storage-ring beam will have the same circular cross-section with a radius of 1.5 mm.

The debunched full momentum spread at 25 GeV scaled from measurements made in the main ring at other energies is $\frac{\Delta p}{p} = 2 \times 10^{-4}$. With 10-turn stacking and a 50% dilution during stacking, the momentum spread in the beam stack will be $(\frac{\Delta p}{p})_{stack} = 3 \times 10^{-3}$. For a main-ring current of 0.14 A (1.8×10^{13} protons) this gives a stack current of 1.4 A.

The maximum transverse dimensions of the beam-stack as given by β_{max} and η_{max} are

(19 mm horizontal) x (7 mm vertical).

In the horizontal plane $\sim$ 34 mm is required for injection and stacking manipulations. Considerations of vacuum, field and alignment error, and space-charge effects add another 20 mm in both planes. Altogether the required "good field" aperature is

(73 mm horizontal) x (27 mm vertical).

Thus, a geometrical aperture of

5 in (h) x 1.5 in (v)

is appropriate. Appendix 2 gives some details of a preliminary design of the magnets, associated power supplies, and a cost estimate of components.

5. Extraction from Main Ring

Since the main-ring long straight E is used for the colliding beams, if the 25-GeV beam is extracted from a long straight, it must be long straight D which is one main-ring sextant or about 1 km upstream from the storage ring. The beam transport line would, then, be very long and expensive. We plan to extract the beam from the upstream end of the second normal cell upstream of long straight E. This is done as follows:

A rather thick current-septum magnet is located in the 7-foot mini-straight, following the F quadrupole. The beam is kicked across the septum by a fast kicker placed 90° betatron oscillation phase upstream. The 20-foot main-ring dipole following the septum magnet is replaced by a C-magnet (Fig. 7). The beam deflected by the septum will exit across the opening of the C-magnet and through

a hole in the yoke of the following main-ring dipole. The parameters of the magnets and the beam geometry are:

Fast kicker

Rise time	< 0.3 μsec
Length	1.5 m
Field	300 G
Kick angle	0.52 mrad

Septum dipole

Septum thickness	1.5 cm
Length	2 m
Field	10 kG

Beam geometry

	displacement from central orbit	angle from central orbit
Entrance to septum	5 cm	0
Entrance to C-magnet	7.5 cm	0.23 rad
Entrance to yoke-hole of following MR dipole	23 cm	.030 rad
Downstream end of MR dipole	44 cm	.038 rad.

A layout of the extraction chain and the injection transport line is shown in Fig. 8.

6. Injection and Stacking

The injection beam transport line is shown in Fig. 8 and is composed of four FODO cells identical to those in the storage ring (unity transfer matrix) to produce a total bending angle of 1.120 rad. Quadrupoles at either ends of the FODO

cells will match the beam into the storage ring. Conventional single-turn kicker injection scheme will be used.

The momentum-stacking scheme, à la CERN ISR, will be used to stack 10 turns in the storage ring. For synchrotron capture at injection, the storage ring rf frequency must equal that of the main ring. This determines the exact length of the injection orbit. After injection the beam is decelerated to the stacking orbit in 1 sec. The storage-ring rf parameters are:

a. γ_t (transition-γ) 6.2

b. Horizontal dimensions at injection kicker (Fig. 4)

η (= η_{max})	3.79 m
Beam stack width	$\frac{\delta p}{p} = 3 \times 10^{-3}$, $\delta x = 11.4$ mm
Separation from injection to central orbits	$\frac{\delta p}{p} = -6 \times 10^{-3}$, $\delta x = -22.7$ mm
Separation from injection to stacking orbits (stacking on "top")	$\frac{\delta p}{p} = -7.5 \times 10^{-3}$, $\delta x = -28.4$ mm, $\delta E = -194$ MeV
Beam width (betatron oscillation)	6.9 mm

c. Orbit length

Injection orbit	581.463 m =	460.091 curved 121.372 straight
Central orbit	581.372 m =	460.000 curved 121.372 straight

d. Frequency

Orbital frequency at injection	0.515246 MHz
Revolution period	1.94 μsec

Harmonic number	103
RF frequency at injection	53.0703 MHz
RF frequency at stacking	53.0801 MHz
RF frequency modulation range	9.8 kHz

e. Voltage

Deceleration time (δE = -194 MeV)	1 sec
Energy gain per turn	-377 eV
Synchronous phase	50°
RF peak voltage	492 V

The rf system is quite simple and modest. Some manipulation of the 25 GeV beam will be done in the main ring before extraction to shape the beam bunches to match that of the rf buckets in the storage ring.

7. Vacuum and Mode of Operation

During stacking only $\sim \frac{1}{10}$ of the main-ring beam for each of 10 pulses is extracted at 25 GeV and injected into the storage ring. The remaining $\frac{9}{10}$ of the beam in each pulse can be accelerated to 400 GeV for other experiments. So there will be no noticeable interference and the storage ring can be recharged rather frequently, say, every 10 minutes. During the 10 minutes with a beam stored in the storage ring the operation of the main ring is totally normal. Colliding-beam experiments are performed from 50 GeV x 25 GeV (see Section 8 below) up to 400 GeV x 25 GeV during the ramp and flat-top of each main-ring pulse. Depending on the main-ring cycle time, the duty factor can be as high as 50%. At the end of 10 minutes the degraded stored beam is dumped and a new beam is stacked from parts of the following 10 main-ring pulses.

To obtain a stored beam life-time of 10 minutes an average vacuum around the storage ring of 10^{-9} Torr is adequate. In the colliding long straight, the beam-gas background must be reduced to a tolerable level for the experiment. There the vacuum must be better than 10^{-10} Torr. Appendix 3 gives some details of the proposed vacuum system and a cost estimate of components.

8. Luminosity and Tune Shift

For head-on collision the luminosity L per unit length ℓ of overlapping beams is given approximately by

$$\frac{dL}{d\ell} = (0.26 \times 10^{30}\ \mathrm{cm}^{-2}\ \mathrm{sec}^{-1}/\mathrm{m})\ \frac{I_1 I_2}{a}$$

where a is the cross-sectional area in cm^2 in which the two beams overlap, and I_1 and I_2 are the beam currents in Ampere contained in the overlap area a. At the mid-point of the colliding straight, the two beams have identical cross-section with area $a^* = \pi(0.128\mathrm{cm})^2 = 0.051\ \mathrm{cm}^2$. Going away from the mid-point, the M.R. beam size remains substantially the same but the storage-ring beam gets larger as

$$a = a^*[1 + (\frac{\ell}{\beta^*})^2]$$

Integrated over the whole length ($\ell = \pm 9\ \mathrm{m} \equiv \pm\ell^*$) of the colliding straight, we get

$$L = (0.26 \times 10^{30}\ \mathrm{cm}^{-2}\ \mathrm{sec}^{-1}/\mathrm{m})\ \frac{2I_1 I_2}{a^*}\ \beta^*\ \tan^{-1}\frac{\ell^*}{\beta^*}$$

$$\cong 10^{31}\ \mathrm{cm}^{-2}\ \mathrm{sec}^{-1}$$

The long-term stability of a beam under the influence of the non-linear beam-beam forces is conventionally characterized by the tune shift. The tune shift of particle 1 travelling unit length through beam 2 is given by

$$\frac{d\delta\nu_1}{d\ell} = (0.32 \times 10^{-3}) \frac{\beta_1}{\gamma_1} \frac{I_2}{a_2}$$

where, as before, β is in m, I in amperes, and a in cm^2. Remembering that (1) for the main ring $a \propto \frac{1}{\gamma}$ and (2) for the storage ring both a and β increase with ℓ as $1 + (\frac{\ell}{\beta^*})^2$, and assuming that particle 1 stays inside beam 2 over the entire length of the colliding straight (hence an overestimate) we get, at different main-ring energies.

Main-ring energy	$\delta\nu$ (main-ring)	$\delta\nu$ (storage-ring)
8 GeV	0.67	0.00014
50 GeV	0.12	0.00075
400 GeV	0.015	0.006

The tune shift of the storage-ring beam attains the accepted limit of about 0.005 only at the peak main-ring energy. Therefore we do not expect instability in this beam due to the beam-beam effect. The tune shift of the main-ring beam is rather large. But since the main-ring beam is not stored for a long time, a tune shift of even 0.12 should be tolerable. We expect that the main-ring beam should be kept away from the storage-ring beam at injection and the two beams could be made to collide for the experiment from 50 GeV on up. To go below 50 GeV the storage-ring beam current may have to be reduced with a corresponding reduction in luminosity.

The large tune shift of the main-ring beam opens up the possibility of doing some experiments to study the long-term stability of beams under the influence of beam-beam effects. This information is crucial for designs of future large colliding-beam storage rings.

IV. Detection Apparatus

1. Kinematics

The interaction of the 25 GeV stored proton beam with the main ring beam of energy E, results in an increasing velocity of the center of mass as the main ring energy is increased from 50 to 400 GeV. We have

$$\frac{1}{\gamma_{cms}} = \frac{2\sqrt{25/E}}{1 + 25/E}$$

Emission of particles at 90° in the cms corresponds to a laboratory angle $\theta_{LAB} = \tan^{-1}\left(\frac{1}{\gamma_{cms}}\right)$. A table of values of θ_{LAB} versus main ring energy E is given below.

E(GeV)	θ_{LAB} (degrees)
50	43°
100	39°
200	32°
300	28°
400	25°

Muons or hadrons emitted at 90° in the cms with transverse momentum $p_{\perp}$, have a laboratory energy $\approx \gamma_{cms}\, p_{\perp} > p_{\perp}$. Thus the laboratory energy of particles is boosted for any given transverse momentum.

This fact is important for calorimetry measurements of the hadronic energy as the resolution improves markedly with increasing energy. Specifically, $\gamma_{cms} \approx 2$ for $E > 300$ GeV and this results in hadronic energies being doubled in the case of emissions at 90° cms and much more than doubled for less than 90° production. As energy resolution is roughly proportional to the inverse square root of hadron energy this provides a minimum of 40% improvement of resolution compared to the equal energy beam situation. Momentum resolution of muons is unaffected by this boost as the use of magnetized iron limits the momentum measurement error to about ± 10% independent of energy. Thus the use of unequal beam energies is advantageous to the minimization of errors in the determination of an imbalance of transverse momentum in $W^{\pm}$ production. In addition there is less problem due to $\pi \rightarrow \mu$ decay in flight thereby allowing direct muons to be more easily identified.

2. General Characteristics

The two beams interact over a field free distance of 17.84 meters. To obtain the maximum effective luminosity we therefore require the detector to span this entire length and be uniformly sensitive to an interaction happening at any point along this distance. The detection criteria are:

a) Muon identification. We ask for close to 100% identification efficiency, independent of the sign of the muon electric charge. In addition, the identification of muons should be effective down to a few GeV muon energy.

b) "Good" quality spatial information. In addition to the measurement of the angle and momentum of the muons, there is substantial physics content in the spatial development

of the hadronic cascade.

c) Energy-momentum information. Muon momentum determination in magnetized iron is limited by multiple scattering to a resolution of about ± 10%. The RMS energy resolution of the hadronic cascades improves with energy, and with the sampling frequency.

3. Detector Concept

The proposed detector is a cylinder stacked from drift chamber and magnetized iron sandwiches. This is shown schematically in Fig. 9. Each iron plate is 10 cms thick and toroidally magnetized. A gap of about 5 cm is provided between adjacent plates for the introduction of detectors, to be described below. The radius of the detector reflects primarily the criteria involved in the trigger as described later. The result is a radius of 1.2 meter which also corresponds to about 5 interaction lengths. Although this does not correspond to total hadron cascade containment necessary for best energy resolution (see Fig. 10) it is adequate at 50 GeV and the situation improves as the energy increases and angles sweep forward. Figure 11 shows the measured hadron energy resolution with 4" steel slabs and scintillator counters. The same data show that the resolution deteriorates by a factor of two when sampling is performed every 8" instead of 4". These measurements were made by the Cal. Tech.-Fermilab neutrino experimental group.[2] The arrangement of 10 cm steel plate and 5 cm gap for detector is repeated 118 times for the full length of 17.84 meters of interaction length.

4. Detector Detail.

We propose using multiwire proportional drift chambers. These devices are intended to provide all of the following capabilities:

a) self triggering

b) accurate localization of tracks to about 1 mm. This is necessary for muon momentum measurements.

c) measurement of the energy of the hadronic cascade, through calorimetry (i.e., pulse height) and track counting. We are aware that proportional chambers have not been used for this purpose in the past. We discuss this point later.

d) provide 3-dimensional (i.e., non-projective) spatial information. This capability should enormously help reconstruction of the events due to absence of the usual ambiguities.

The basic idea is shown in Fig. 12. Two chamber cells constituting one module will be needed per gap to resolve the left right ambiguity problem. The wire spacing will be 5 cm and the overall length 2.4 m. Thus 88 wires are required per module. In the first phase of the experiment we will have the detectors in alternate gaps separated by 20 cm. This implies a total of 5,192 wires in the system. Each module is rotated by 60° with respect to the adjacent module. This provides the maximum spatial resolution for muon momentum analysis at any azimuthal production angle. Calorimetry information is derived from the pulse area information. It is proposed to record the pulse area individually for each end of each wire. Thus, not only can the local energy deposition be measured, but the

position of the discharge along the wire can be determined by the current division method. Thus each cell would provide a three dimensional spatial datum plus an energy datum.

We estimate that the balance of transverse momentum will be checked in a given event to better than a few GeV. This is very much less than the imbalance ($\sim M_W/2$) produced by the lack of detection of a neutrino in massive W production and decay.

Along the wire, the resolution obtained by the current division technique may be limited in practice to about 1% of the wire length. In the present case, this would be about 2 cm. This is small or comparable to the radius of a hadronic shower.

The design of the circuitry needed to accomplish these purposes represents a significant developmental effort. The requirements are technically straightforward, and the main challenge lies not in producing a workable circuit but in keeping the costs low. A circuit with the required specifications has been built at L.B.L. by D. Nygren. Electronics for the system will likely be in the $30/channel range.

Calibration of pulse height and circuit performance monitoring can be accomplished by incorporating simple strip lines within the chamber's end regions. A pulse travelling along these lines will capacitively induce a signal on the sense wires; the pulse height and time delay can be computer controlled, and a test can be made every main ring cycle during the period when there is no beam in the main ring.

Scintillation counters will be inserted in every 6th gap (i.e., every 0.9 meters) to provide good time resolution. At each end of the 17.8 m detector a scintillation counter hodoscope will be used.

5. Calibration of Detector.

The detector is self-calibrating in a continuous fashion, as far as muons are concerned. Due to the 10 cm granularity of the steel plates a 10 GeV muon has its energy determined by range to an accuracy of about ± 1% (or ± 2% when sampling every second gap). The momentum calibration and associated systematic errors can then be checked throughout the course of the experiment using muons which stop in the detector.

It may also prove useful to insert in the main ring beam some meters upstream of the detector, a rotating carbon target of the type used at C0. Muons and hadrons produced in the target could then be momentum analyzed in magnet B (see Fig. 6) and be used to calibrate the detector.

6. Detector Development

Proportional drift chambers have never been used for hadron calorimetry in the past. Although there is some evidence that a linear dynamic range of 100:1 can be obtained we intend doing a simple test to check this behavior. We propose constructing a single 1' x 1' proportional drift chamber and operating it behind 10 to 20 cm of steel (see Fig. 10) with 100 GeV hadrons incident on the steel. In this way, the effective response of the detector at the peak of the hadron cascade can be studied. We require good detection efficiency for single minimum ionizing particles (muons) at the same time. The technique required to achieve an adequate dynamic range will be investigated.

V. Trigger and Event Rates

1. Trigger

With a luminosity of 10^{31} cm^{-2} sec^{-1} and a proton proton total cross section of 50 mb, the total number of beam beam interactions per second is 5×10^5. Thus, a selective trigger is required to reduce this number to a manageable rate (say $< 10^3$/sec) for recording data on magnetic tape.

There are three geometrical possibilities for a muon produced directly or from the decay of hadrons. These are:

a) The muon may stop within the detector.

b) The muon may leave from the side of the detector.

c) The muon may leave from the end of the detector.

For the moment we neglect the bending of the muon trajectory due to the magnetized iron slabs and return to that later.

Case a), in which the muon stops within the body of the detector, is the simplest case. For the given energy of the muon its transverse momentum must have been less than 1 GeV/c, otherwise it would have traversed the radial thickness of steel in the detector. A transverse momentum of $\geq$ 1 GeV/c is a useful trigger level, because, the fraction of all produced pions which have $p_\perp > 1$ GeV/c is $\sim 5 \times 10^{-3}$ and the probability of a pion with $p \geq 1$ GeV decaying to a muon in a reasonable distance is $\lesssim$ 0.5%. Hence

$\sim 2 \times 10^{-5}$ of the produced pions in an interaction will give rise to a muon with $p_\perp \gtrsim 1$ GeV/c. Therefore, in case a) the muon has $p_\perp$ less than 1 GeV/c, and we do not wish to trigger on such events.

Case b), in which the muon leaves the side of the detector, is obviously of interest, because the muon has a transverse momentum $\gtrsim 1$ GeV/c. The trigger would involve a minimum of several adjacent drift chamber modules having recorded a particle, the last one having fired its outermost wire. The chance that a high $p_\perp$ hadron would penetrate 1.2 meters of steel is not negligible. On the other hand, these events are sufficiently rare that they will not overload the trigger and be of interest in themselves.

Case c), in which the muon leaves from the end of the detector, is non trivial because of the lack of knowledge of either the muon energy or its transverse momentum. However, we may proceed in the following way. An event is identified in which a particle has left the detector from one of the two ends. A requirement is then made that a minimum of 6 m at the end of the detector has recorded tracks. Hadronic cascades from the event are expected to be mostly over a radius of $\lesssim 2$ meters (see Fig.10) around the interaction point and therefore do not confuse the situation too much. If, indeed, 6 meters of detector has fired, including at least 6 scintillation counters, this corresponds to a 6 GeV muon and we would require that the position of the track as it exists from the end is near the outer edge of the detector. The angle of the muon in this case would be about 10° in the laboratory and $p_\perp \approx 1$ GeV/c. As the length of

detector over which tracks have been recorded increases beyond 6 m ($\equiv$6GeV) a corresponding reduction in the radial distance of the muon exiting point from the beam axis can be tolerated. This means we allow the minimum $p_\perp$ in the trigger to go below 1 GeV/c as the muon momentum increases and the corresponding probability of decay in flight for hadrons goes down. We maintain the rejection of hadron decay to muons at the level of about 2×10^{-5} in this way.

The trigger rate from pion decay in flight is then

$$5 \times 10^5 \times 15 \times 2 \times 10^{-5} = 150/\text{second}$$

where 15 is the approximate number of charged pions produced in an interaction. The inclusion of the effect of magnetization of the iron slabs tends to raise the minimum $p_\perp$ in the trigger for one sign of muon charge and correspondingly lower it for the other sign. These effects are relatively small and do not greatly affect the trigger rate.

The single muon trigger with $p_\perp \gtrsim 1$ GeV/c is simple and efficient for studying the production and leptonic decay of the $W^\pm$ and Z^o mesons. It is possible that the transverse momentum characteristics of the hadrons, from hadronic decays of these particles, are so dramatic that a trigger can be developed for their study also. We have not investigated this latter possibility in any detail.

2. Event Rate for $W^\pm$ Detection.

Existing results for lepton pair production seem to fall on a smooth curve suggesting that the scaling limit may have been reached. If this is the case, then a rigorous lower bound

for the production cross section of $W^{\pm}$ can be given. Secondly, the parton model (without color) gives a good description of the shape of the above scaling function and in addition its absolute magnitude. Inclusion of color changes the predictions by a factor of three. In any case, the fact that the data indicates scaling suggests that these lower limits for $W^{\pm}$ production are probably reliable.

Several factors go into the discussion of the rates and we briefly identify each of these.

a) Luminosity (L). The luminosity is a function of center of mass energy due to the slow spatial contraction of the accelerating main ring beam. We have taken

$$L(E_{MR}) = \frac{E_{MR}}{400} \times 10^{31}\ \mathrm{cm}^{-2}\ \mathrm{sec}^{-1}.$$

b) Cross Section $\sigma(E_{MR})$. We have taken the cross section for W production as described earlier.

c) Acceptance $A(E_{MR})$. We consider 45° as the maximum reasonable angle (in the "forward" hemisphere) for good muon identification and momentum analysis. The minimum angle is quite small ($\lesssim 3^{\circ}$) and does not significantly affect the acceptance. Thus at $E_{MR} = 50$ GeV we cover a little more than the forward hemisphere, while at $E_{MR} = 400$ GeV the acceptance is essentially complete. The acceptance, therefore, is always greater than 50% and increases slowly with E_{MR} up to close to 100%. We have attempted to include the effect of this varying acceptance as a function of E_{MR}.

d) Leptonic Branching Ratio, B. No reliable estimates exist for this number, although a great many guesses have been made which suggest significant leptonic decays should exist. We have taken

$$B = \frac{\Gamma(W \to \mu + \nu)}{\Gamma(W \to \text{all})} = \frac{1}{3}$$

A lower limit for the detection rate of single muons from the production W meson of a given mass M_W may then be calculated. The rate is given by

$$R(M_W, E_{MR}) = L(E_{MR}) \cdot \sigma(M_W, E_{MR}) \cdot A(E_{MR}) \cdot B$$

We have assumed normal machine operation with a 6 second cycle with 1 second flat top. Interaction of the two beams will occur from 50 GeV up to 400 GeV including the flat top portion of the ramp. Inclusion of interactions during the flat top period changes the rates by less than a factor of two. In Figure 13 we show the lower limit to the W event rate, $R(M_W, E_{MR})$, per week per 40 GeV interval of main ring ramp. We have assumed the average 100 hours per week of successful main ring operation.

Integration of $R(M_W, E_{MR})$ over the main ring cycle gives the lower limit of the total number of W events detected/week. The result is shown in the table below.

Mass of W(GeV)	Lower limit of detected $W \to \mu\nu$ events/week
20	630
40	245
60	85
80	25
100	6

Although an event rate of 1/day for 100 GeV massive W's is low, the event will be spectacular and have essentially no background. We therefore believe that the mass range 20-100 GeV can be successfully explored in the manner described. For example, in a three month run we would obtain several hundred W events of the Weinberg Salam type (M_W = 70 GeV).

3. Other Reactions.

1. Muon Pair Production

The predicted lower limit of the $W^{\pm}$ production cross sections rests on the existence of a scaling behavior of the reaction

$$p + p \to \mu^+ + \mu^+ + \text{anything}.$$

It is therefore of great importance that we measure this reaction during the course of the W search. Scaling implies that the dimensionless cross section, $M^3 \frac{d\sigma}{dM}$, for dimuon production is a function of s/M^2 where M is the dimuon mass. Figure 1 shows the available data and a parton model

prediction. The cross section is large. For $s = 4 \times 10^4$ GeV^2 this implies dilepton masses up to 10 GeV can be measured. The scaling properties of the dimuon production can therefore be investigated over a wide range of s and M^2, specifically

$$5 \times 10^3 \leq s \leq 4 \times 10^4$$

and

$$4 \leq M^2 \leq 10^2$$

which implies the range $50 \leq s/_M{}^2 \leq 10^4$ will be measured.

2. J/ψ Production

Experiments at FNAL have shown that magnetized iron is adequate to resolve the J/ψ from the dimuon continuum. We therefore expect to be able to study the production of J/ψ. The total cross section for J/ψ production will be about 5×10^{-7} of the total proton proton cross section assuming no relative increase at higher energy. The event rate will then be

$$5 \times 10^5 \times 5 \times 10^{-7} = 0.25/\text{sec.}$$

Thus, there will be one J/ψ event detected in each main ring ramp. The associated hadronic structure of these events will be measured and may be interesting. In addition, anomalous leptonic decay of new particles produced in association with the J/ψ will be detected as a three, or more, muon event.

3. We will not discuss the many other possible types of measurements such as jet production, multiplicity, etc. which can possibly be performed.

4. Backgrounds.

There are two kinds of backgrounds. These are the rate of single events in the detectors due to the environment of the main

ring tunnel, independent of the small storage ring, and secondly, the background trigger rate due to either single beam effects or cosmic rays. We discuss each of these in turn.

a) Singles Rate in Detectors in the Main Ring Tunnel.

The number of minimum ionizing particles/cm^2/sec/10^{13} protons at 300 GeV and 1 meter from the beam has been measured as 10^4. This measurement was made at C0 with an average beam line gas pressure of 2×10^{-6} Torr. The background has been observed to vary linearly with the pressure in the range 10^{-7} Torr to 10^{-5} Torr. Thus, at an average pressure of 10^{-7} Torr we have 7×10^6 particles/m^2/sec/1.4×10^{13} protons. This rate would be uncomfortably high. Of course, we plan to have a pressure of 10^{-10} Torr in straight section E and in addition use beam scrapers which have proven to be very useful at C0 to reduce backgrounds. In this way, we expect the background rate due to single beam effects to be substantially reduced, and be dominated by the 5×10^5 beam beam interactions per second.

These interactions are distributed approximately uniformly along the 17.8 meters of the detector. The hadronic products of an interaction are contained within about 2 meters along the detector. The reaction rate per 2 meters is $5/9 \times 10^5$/sec. The sensitive time of the proportional drift chamber is determined by the maximum 2.5 cm drift distance. At 200 n sec./cm., the detector

sensitive time is 0.5 μ sec. Hence the probability of two events occurring in the same 2 meter lengths within the drift detector sensitive time is $5/9 \times 10^5 \times 0.5 \times 10^{-6} \sim 3\%$. This is low enough to ensure clean event identification.

b) Cosmic Ray Trigger Rate.

As stated above, we expect to achieve the situation where the singles rates are dominated by beam beam interactions. We therefore anticipate that single beam effects will not lead to a substantial background trigger rate. Discussions with A. Mann of E-1A suggest that cosmic ray backgrounds in the trigger can be eliminated by requiring a total energy loss in the detector of greater than 2 GeV. The single muon trigger, which we have discussed, comes close to satisfying this criterion. It may be useful to require, in addition to the muon trigger as we have defined it, an energy loss in the entire detector of a few GeV. On the basis of experience with cosmic rays triggering the neutrino detectors at FNAL, it seems there will be little problem in restricting their triggering the proposed detector.

VI. Cost Estimate and Schedule

1. Cost Estimate

Detailed cost estimates for the various major components of the proposal are given in the appendices. A summary of that information is provided below:

1.	Conventional construction of the tunnel and experimental room (Appendix 1).	$ 1.09 M
2.	Storage ring magnets including insertions and injection (Appendix 2).	1.26 M
3.	Power supplies and buss work (Appendix 2).	0.38 M
4.	Vacuum system (Appendix 3).	0.35 M
5.	Detection equipment (Appendix 4).	0.57 M
6.	Miscellaneous (Appendix 6).	0.30 M
	Total	$ 3.95 M

We would like to comment on the reliability of these figures. There are two major items, namely 1. and 2. The Architectural Services Division of F.N.A.L. has performed the cost estimate that is given here and the experience in the past has shown that these estimates are usually 10 to 20% high. The second item, i.e., magnet construction, is being put out for bid and we will shortly receive cost estimates from industry. At that stage the overall cost will be reliably established and we anticipate that the above estimates will be justified.

2. Schedule.

It is our schedule to have colliding beams two years from time of approval. The schedule for major components is shown in the table below:

Time	0	1st year	2nd year
1) Conventional Construction	→		
2) Extraction system from M.R.	Design. Construction.	Test →	
3) Transport and injection	Design. Construction.	Install. Test →	
4) SSR magnets and vacuum	Design. Construction.	Installation. Test →	
5) Detector	Design. Construction.	Installation. Test →	
6) W Detection			→

The installation of all components in the tunnel during the second year is greatly facilitated by having access to the tunnel 24 hours per day and seven days per week. This is accomplished by the erection of a modest 6 foot thick concrete block wall at the interface of the tunnel with the main ring. This procedure has been used successfully at CO during the recent installation of the spectrometer in the new room adjoining the tunnel.

VII. Future Development Phases

There are three phases of possible future development of the facility. These are a) having several simultaneous experiments at the interaction region; b) a factor of 10 increase in luminosity to 10^{32} cm^{-2} sec^{-1} and c) increase of center of mass energy up to 400 GeV. We briefly discuss each in turn.

a) Experience with the experimental program at CO has shown that several experiments can operate simultaneously when using the same target. We expect a similar situation to develop

with the interacting beams at straight section E. For example, it appears possible to study Coulomb scattering to measure the real part of proton proton scattering, small angle nuclear elastic scattering and the diffractive inelastic scattering simultaneously with the proposed experiment for W production. A rich and diverse experimental program is likely to develop in the future around the proposed straight section.

b) This proposal has been based on the existing intensity and emmittance of the beam in the main ring. Various improvement programs, currently underway, are expected to increase the current of the beam to its design value of 5×10^{13} protons per pulse. It is therefore possible that the stacked current can be increased to 3 or 4 amps within the same emmittance and be allowed to interact with 5×10^{13} protons per pulse in the main ring. The luminosity in this case would be about 10^{32} cm^{-2} sec^{-1}. The larger tune shift to the main ring beam due to the beam beam interaction would restrict collisions to energies greater than 150 GeV. It may also be possible to use a low β insertion in the main ring to increase the luminosity further.

c) Our schedule is to achieve 200 GeV in the c.m.s. two years after approval. This will be earlier than operation of the energy doubler in the main ring tunnel. However, when reliable operation of the doubler is achieved we could then implement the second phase of the experiment. At a minimum cost and short disruption of colliding beam operations, we could raise the small storage ring by several feet and obtain collisions

with the 1000 GeV beam. This would provide collisions at over 300 GeV in the c.m.s. A much more attractive possibility at that stage, however, involving greater expense and disruption, would be to replace the conventional small storage ring by a superconducting storage ring at 50 GeV and obtain collisions at over 400 GeV in the c.m.s.

These discussions show that a rich and continuing experimental program can be expected to develop around the interaction region where eventually we can hope to achieve a luminosity of 10^{32} cm^{-2} sec^{-1} at over 400 GeV in the c.m.s. This program would develop over the years without significant interference to the rest of the laboratory experimental program.

VIII. Conclusions

We have proposed an experiment which will test the underlying theory of weak interactions in a unique way and establish if a new energy scale in the range 20 to 100 GeV exists. The equipment cost of approximately 1.4 M per year for two years is similar to other major experiments performed at FNAL or the European SPS. We request prompt approval to proceed rapidly with construction of Phase 1 of the experiment which will give 200 GeV in the cms and a luminosity of 10^{31} cm^{-2} sec^{-1}. In the second phase of the experiment we will achieve 400 GeV in the cms and explore masses up to 200 GeV with a luminosity of 10^{32} cm^{-2} sec^{-1}.

References

[1] S. Pakvasa, D. Parashar and S. F. Tuan, Phys. Rev. D 10 2124 (1974).

[2] F. J. Sciulli, CALT 68-502.

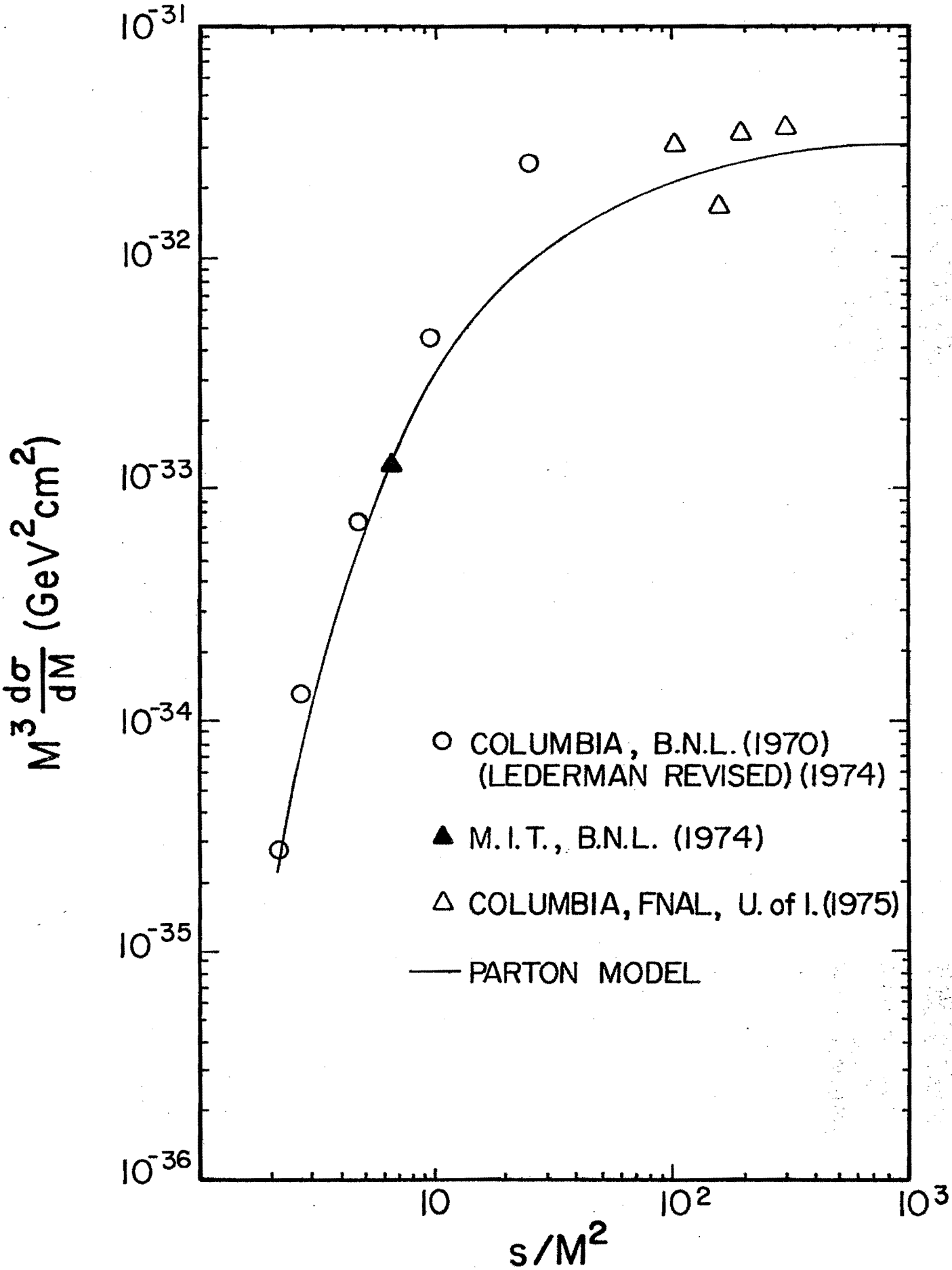
10^{-31}
10^{-32}
10^{-33}
10^{-34}
10^{-35}
10^{-36}
$M^3 \frac{d\sigma}{dM}$ (GeV^{2}cm^2)
10
10^2
10^3
s/M^2
COLUMBIA, B.N.L. (1970)
(LEDERMAN REVISED) (1974)
M.I.T., B.N.L. (1974)
COLUMBIA, FNAL, U. of I. (1975)
PARTON MODEL

FIG. 1

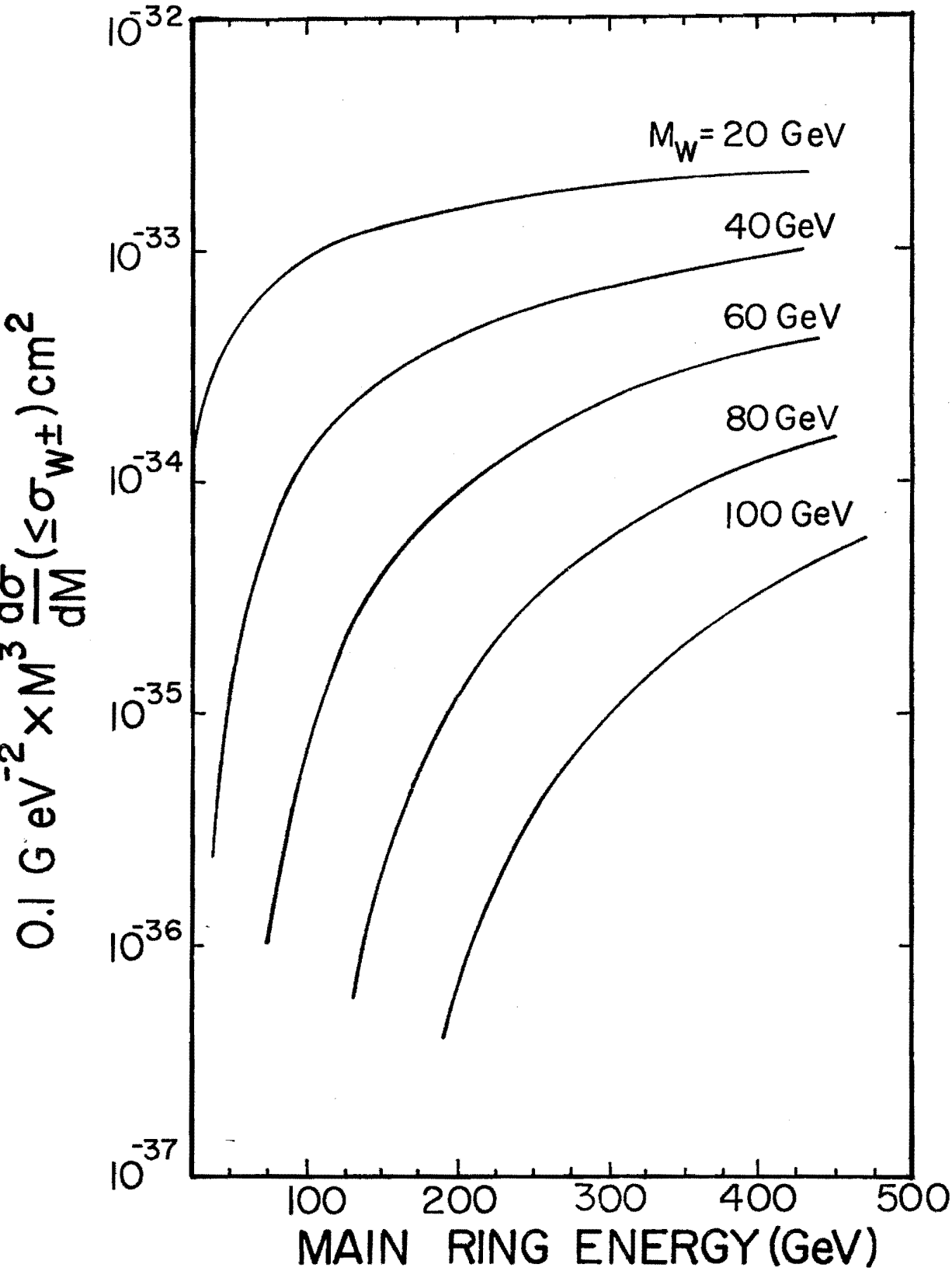
10^{-32}
10^{-33}
10^{-34}
10^{-35}
10^{-36}
10^{-37}
M_W = 20 GeV
40 GeV
60 GeV
80 GeV
100 GeV
$0.1\ GeV^{-2} \times M^3 \frac{d\sigma}{dM}(\leq \sigma_{W^\pm})\ cm^2$
100
200
300
400
500
MAIN RING ENERGY (GeV)

FIG.2

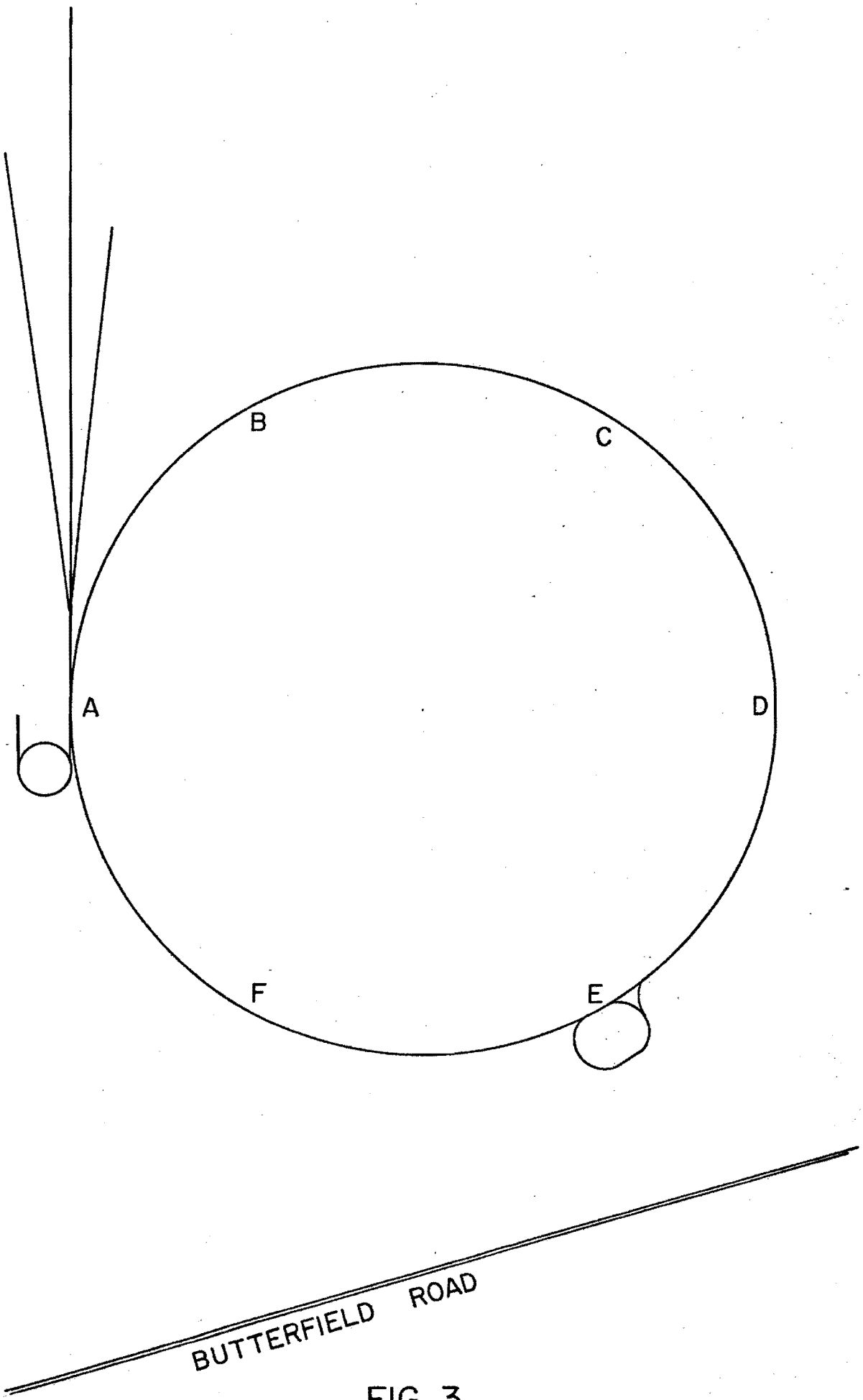

FIG. 3

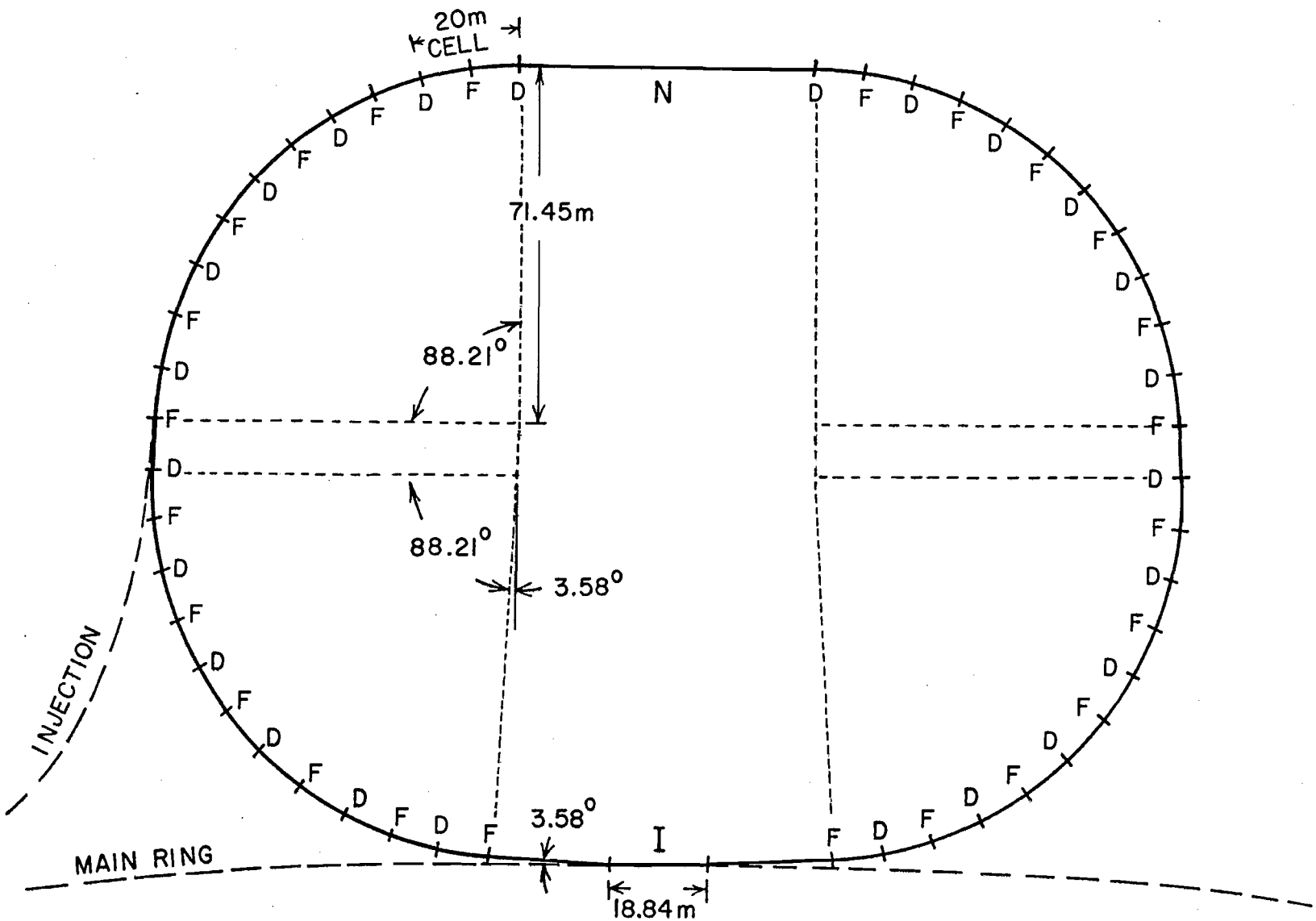
20m
CELL
N
I
71.45m
88.21°
88.21°
3.58°
3.58°
18.84m
INJECTION
MAIN RING

FIG. 4

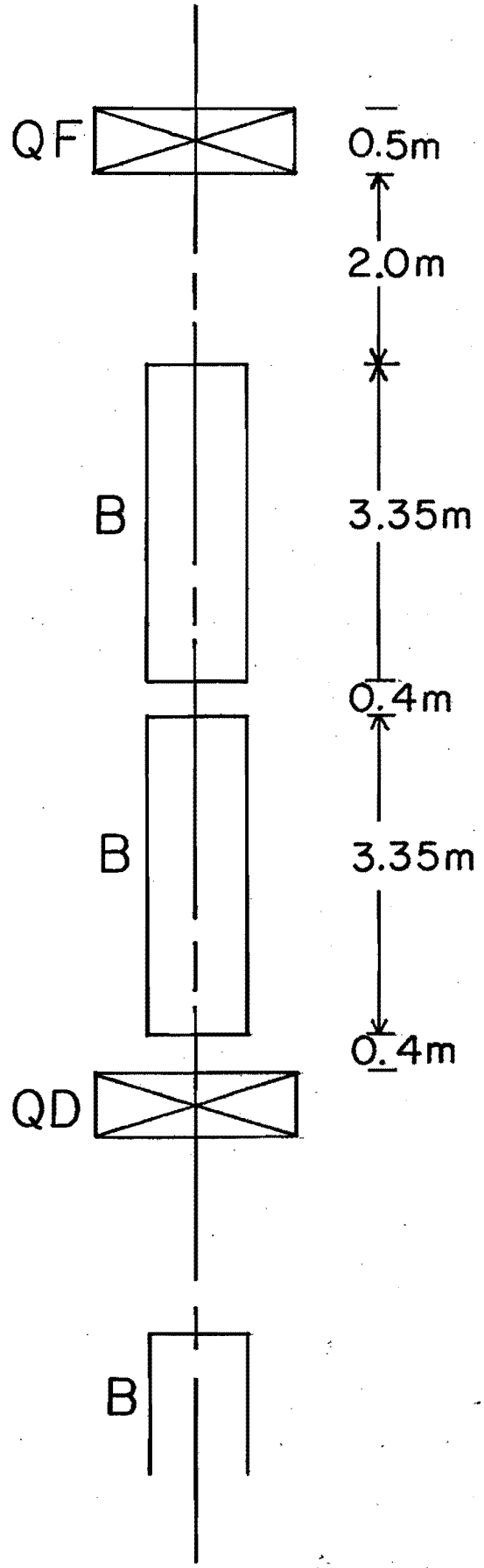

FIG. 5

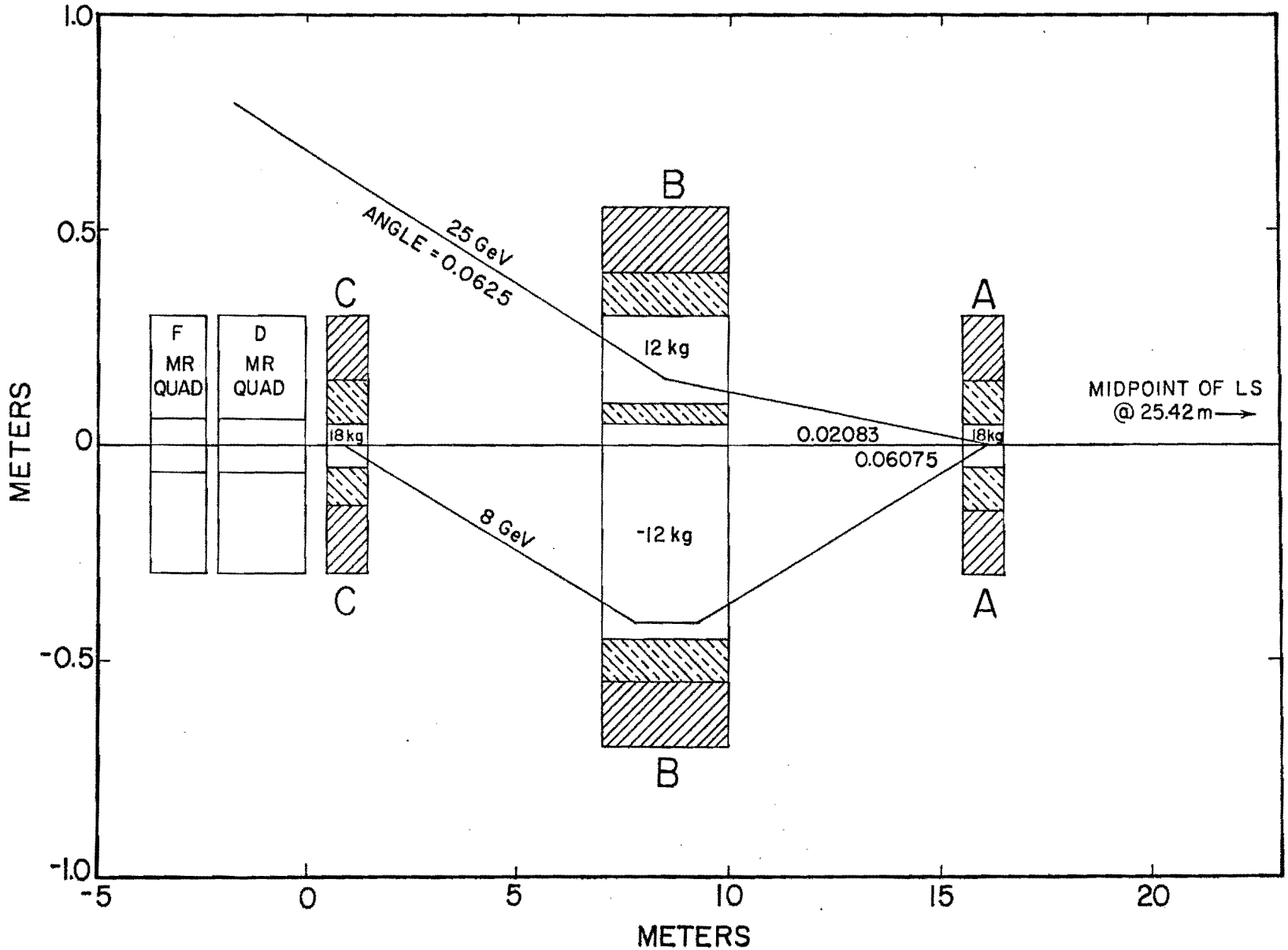
1.0
0.5
0
-0.5
-1.0
METERS
-5
0
5
10
15
20
METERS
F
MR
QUAD
D
MR
QUAD
C
C
B
B
A
A
18 kg
12 kg
-12 kg
18kg
25 GeV
ANGLE = 0.0625
8 GeV
0.02083
0.06075
MIDPOINT OF LS
@ 25.42 m

FIG. 6

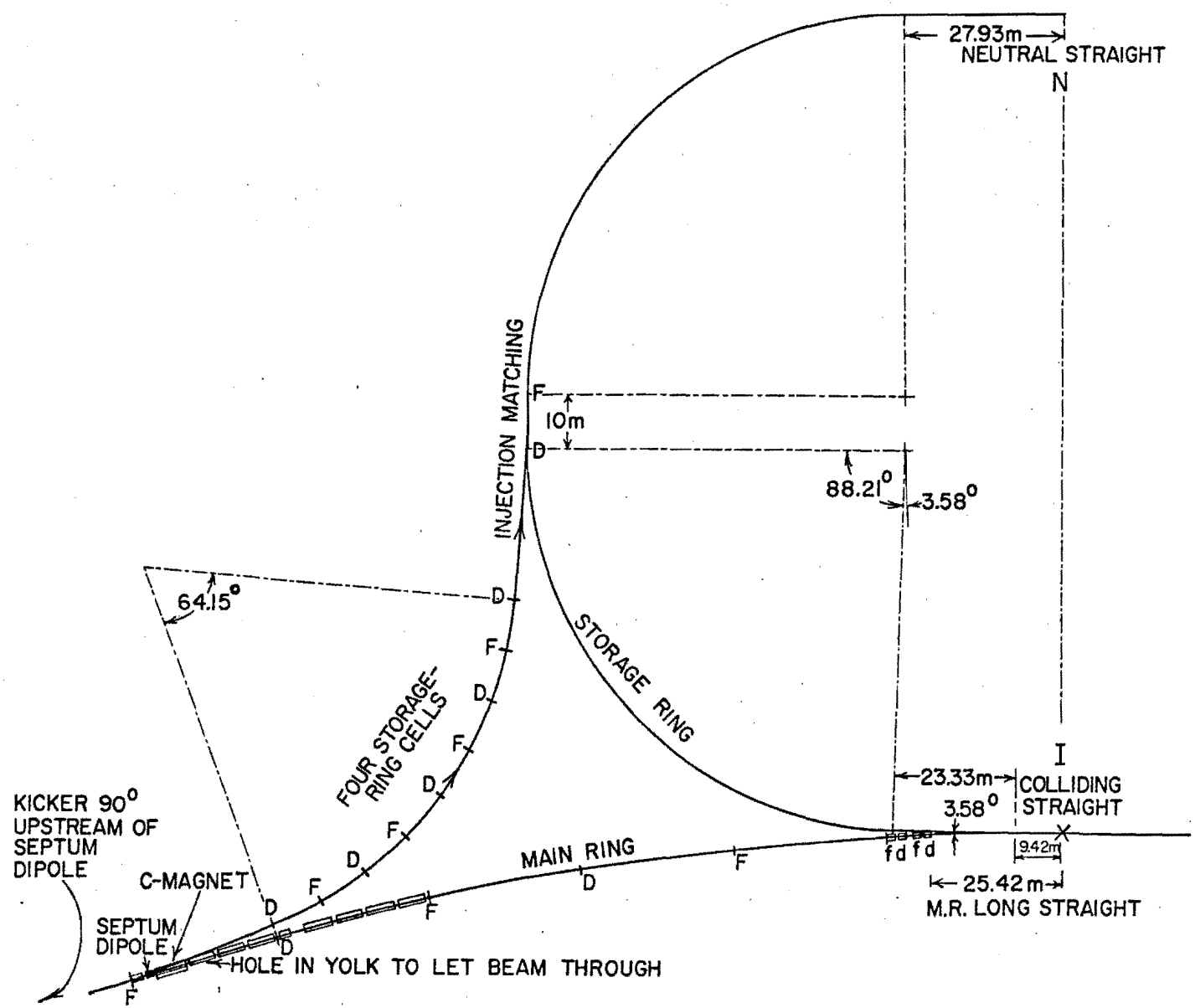
27.93m
NEUTRAL STRAIGHT
N
INJECTION MATCHING
F
10m
D
88.21°
3.58°
64.15°
D
F
D
F
D
F
D
F
D
F
D
F
STORAGE RING
FOUR STORAGE-RING CELLS
KICKER 90° UPSTREAM OF SEPTUM DIPOLE
C-MAGNET
SEPTUM DIPOLE
HOLE IN YOLK TO LET BEAM THROUGH
MAIN RING
I
23.33m
COLLIDING STRAIGHT
3.58°
fd fd
9.42m
25.42m
M.R. LONG STRAIGHT

FIG. 8

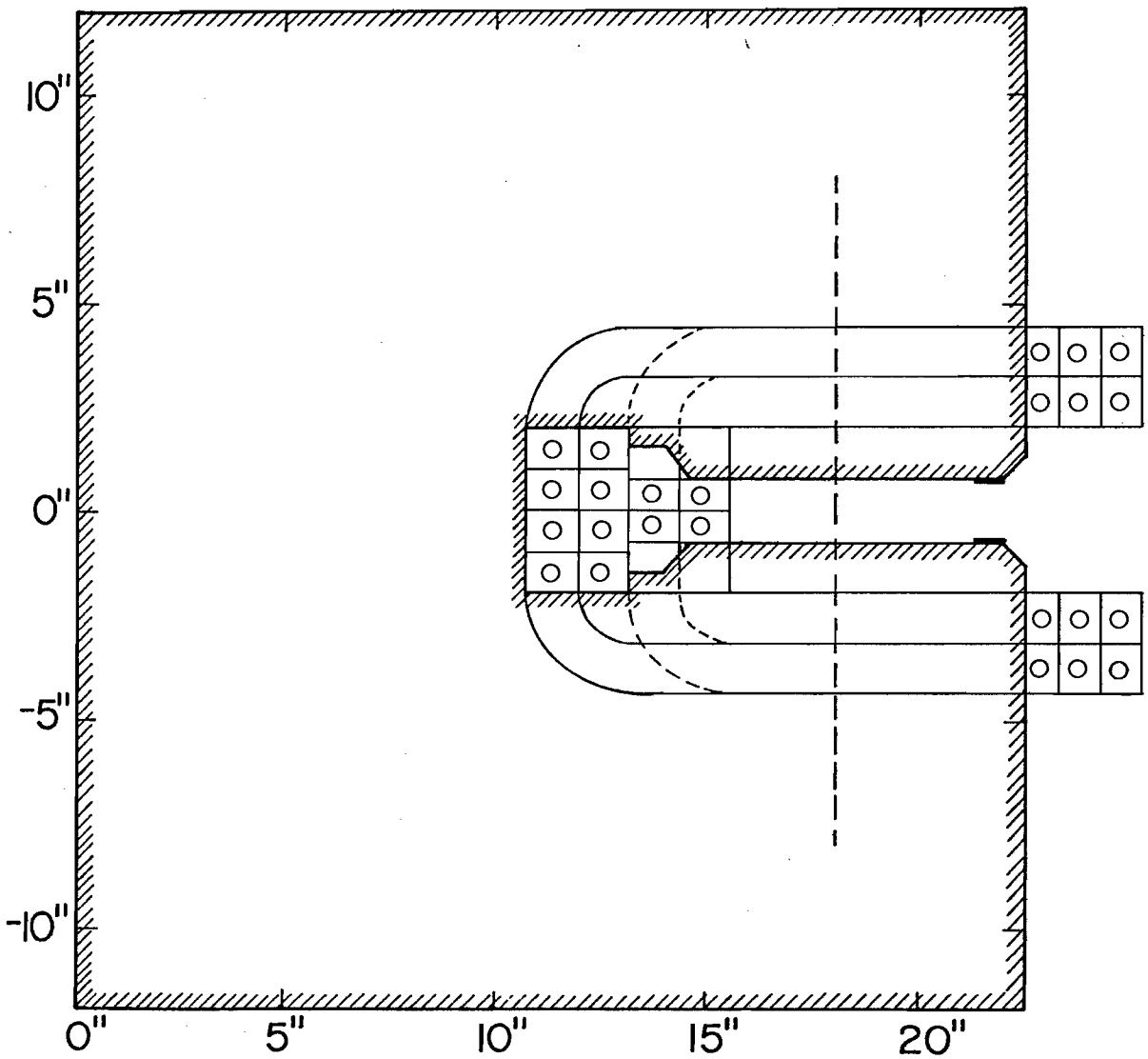

FIG. 7

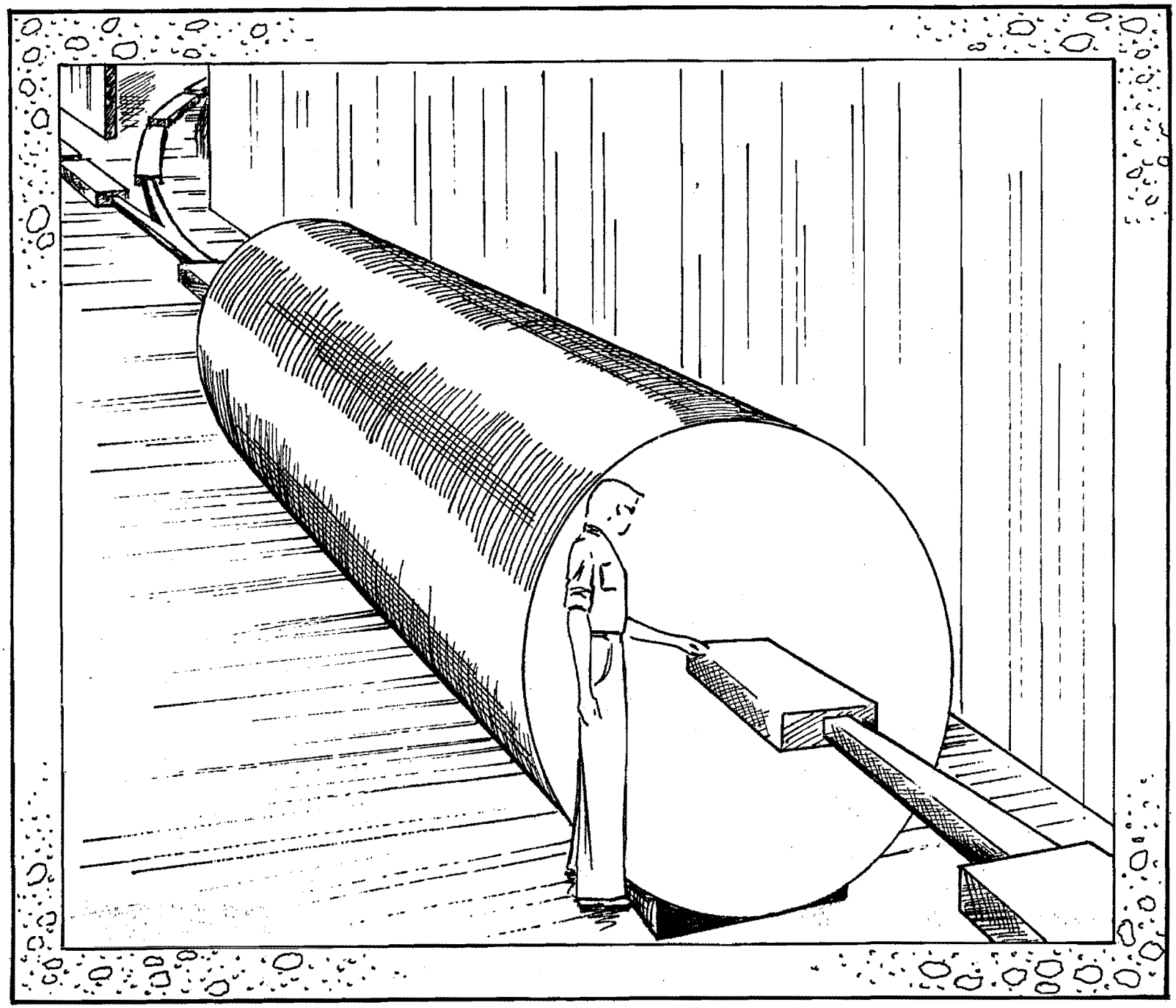

FIG. 9

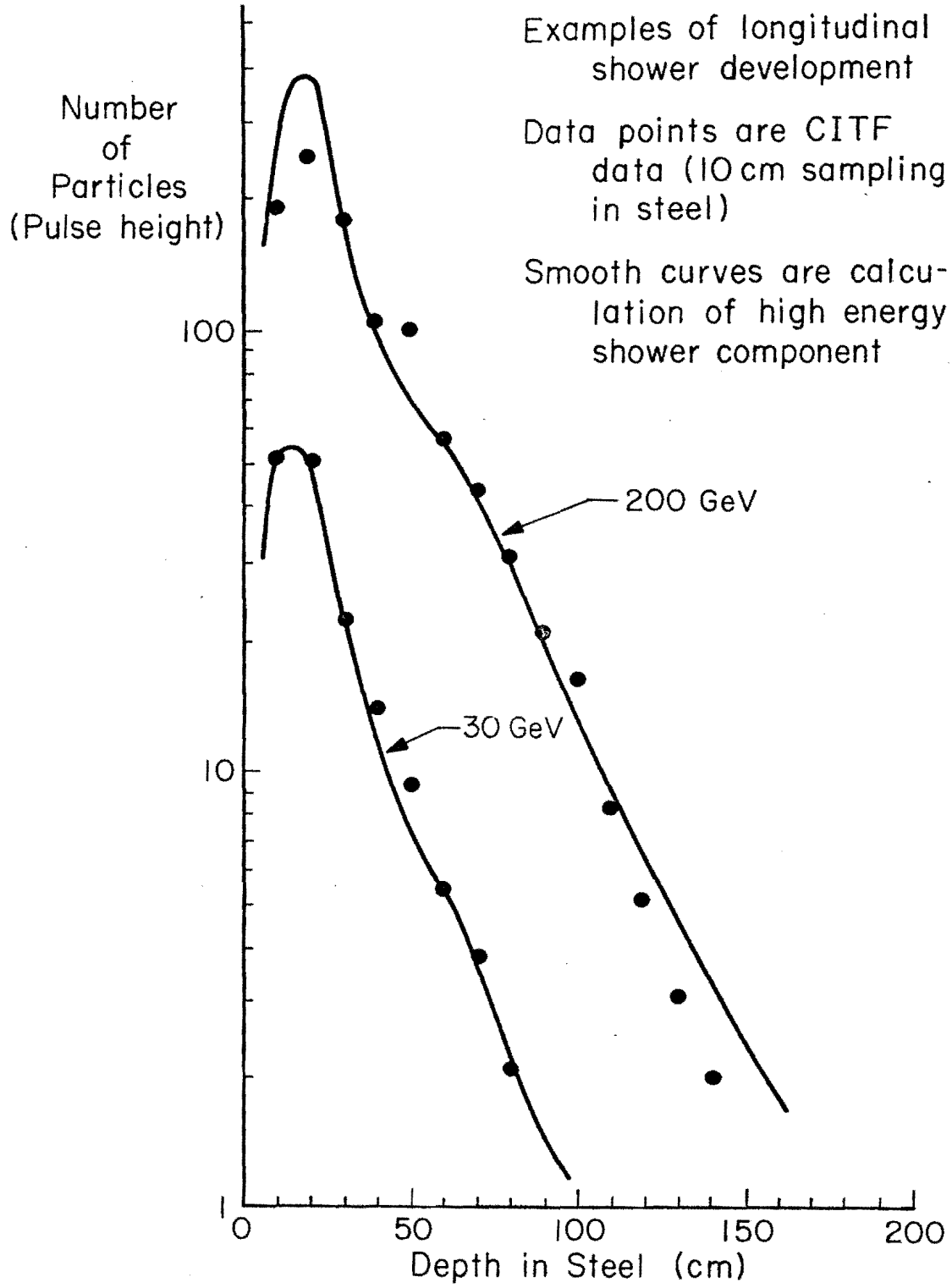

CITF calorimeter response vs. depth in steel.

FIG. 10

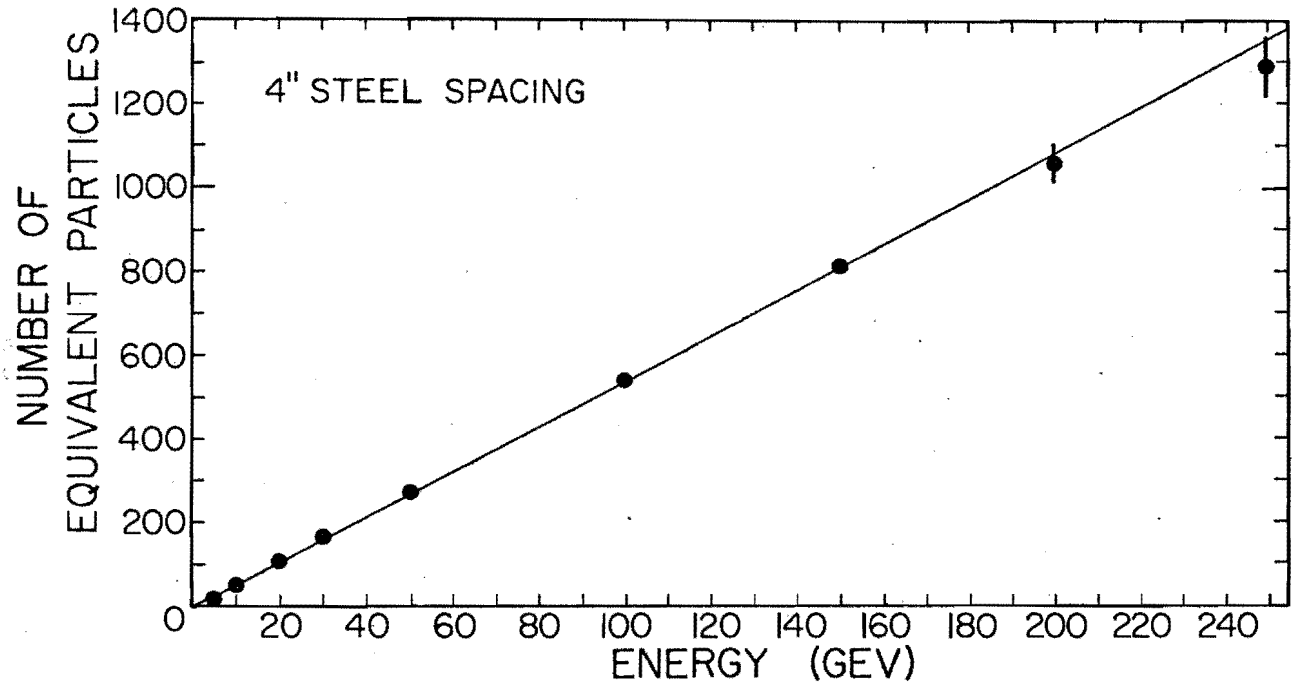
4" STEEL SPACING
NUMBER OF EQUIVALENT PARTICLES
0
200
400
600
800
1000
1200
1400
20
40
60
80
100
120
140
160
180
200
220
240
ENERGY (GEV)

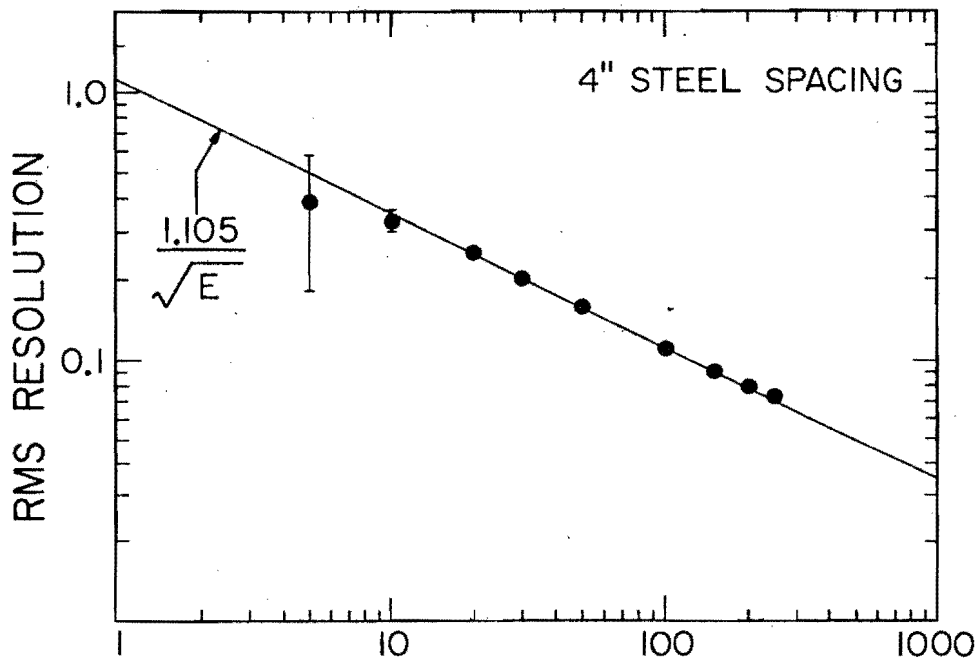
4" STEEL SPACING
RMS RESOLUTION
1.0
0.1
1.105
√E
1
10
100
1000

FIG. 11

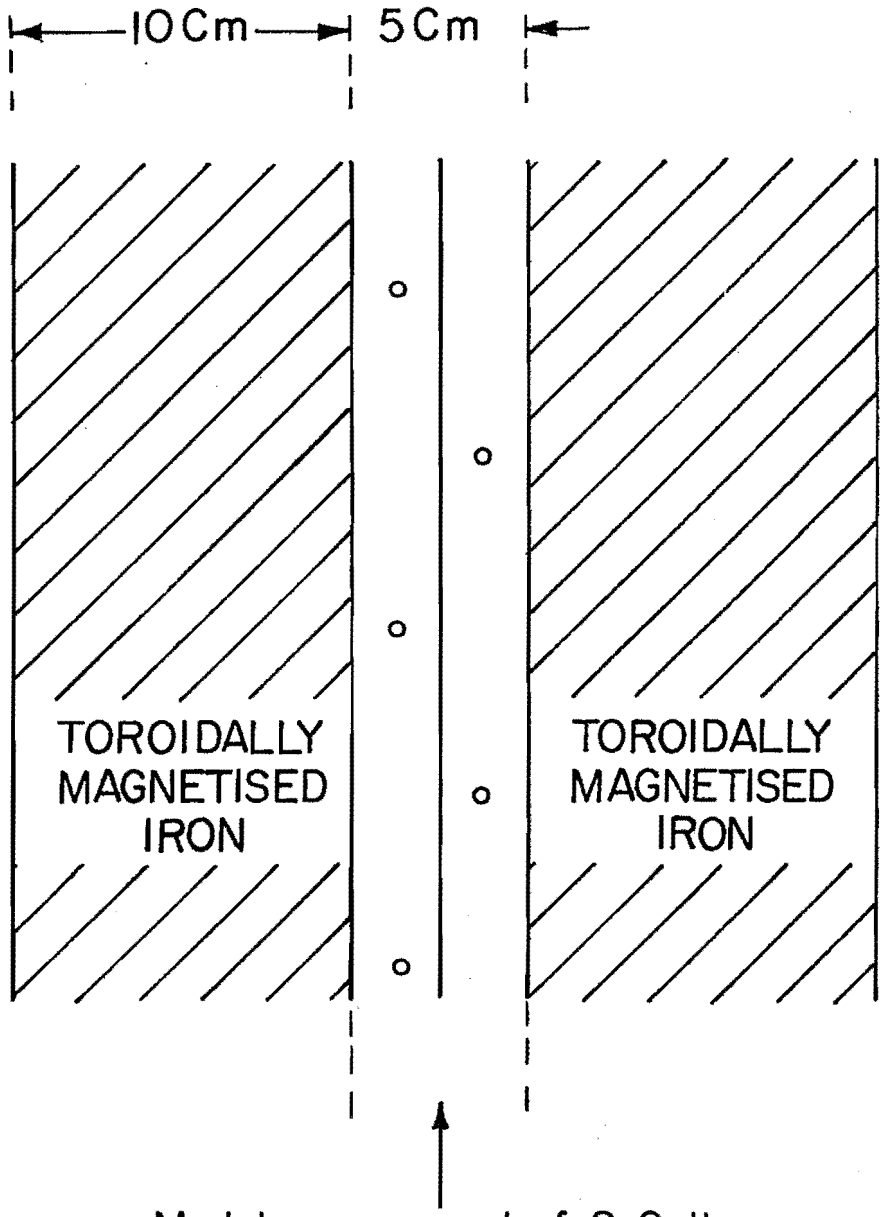

Module composed of 2 Cells of Drift Chambers with 5 cm wire spacing. Cells are staggered to avoid left right ambiguity.

FIG. 12

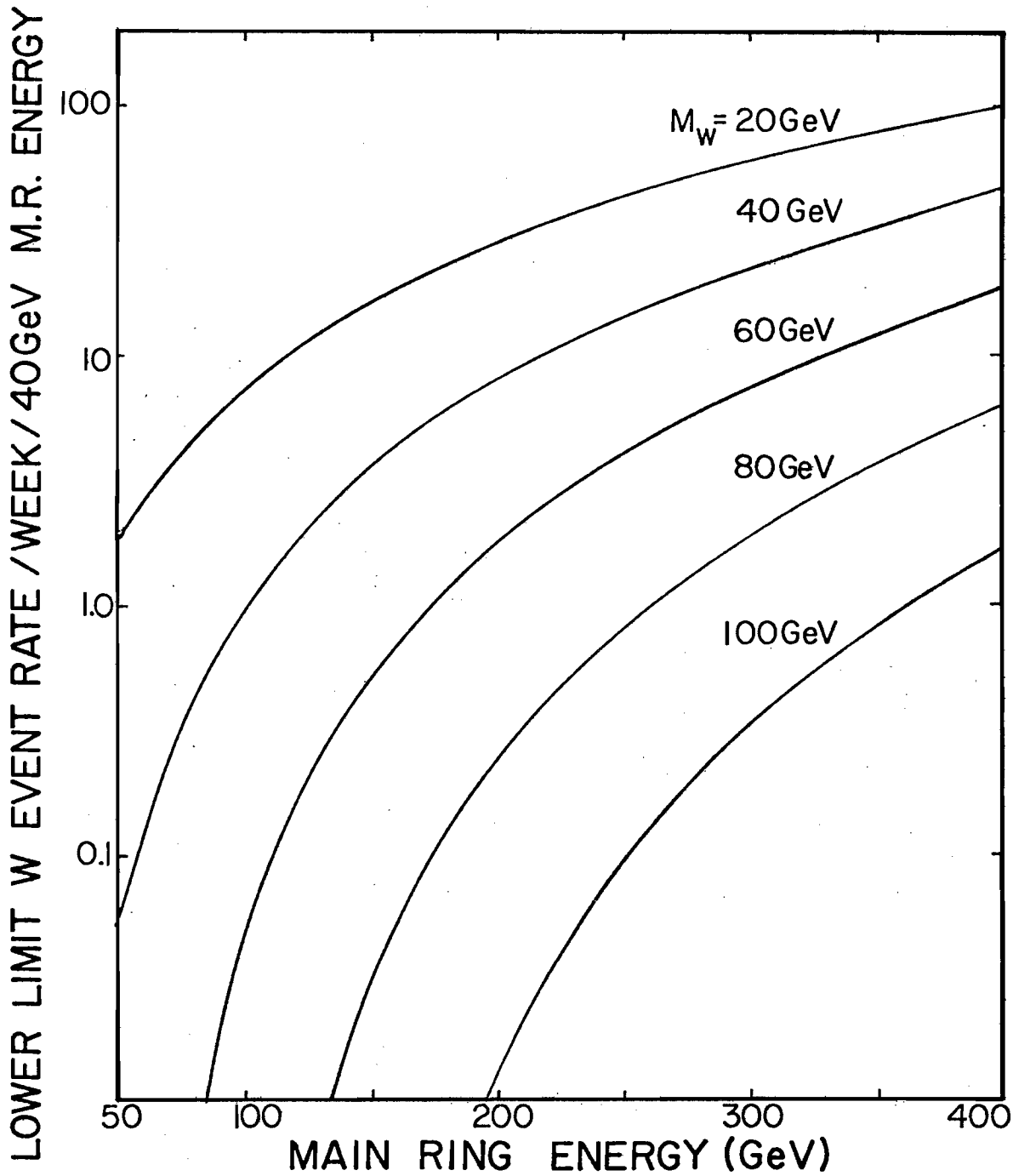
LOWER LIMIT W EVENT RATE /WEEK/ 40GeV M.R. ENERGY
100
10
1.0
0.1
M_W= 20GeV
40 GeV
60GeV
80GeV
100GeV
50
100
200
300
400
MAIN RING ENERGY (GeV)

FIG. 13

Appendix 1

Tunnel and Experimental Hall Conventional Construction

The proposed location for the 25 GeV/c storage ring is E0 straight section. Some of the advantages of this area are:

1. There is very little apparatus in the E0 straight section.
2. The service building at E0 is essentially empty, making it available for a Control Room and Experimental Counting Room.
3. E0 has a ramp entry making access with equipment easy.
4. The earth level at E0 minimizes earthwork. (∿740' ± 2', main ring berm is 752' 6", main ring tunnel floor is 722' 6", the proposed ring floor is 725').

Figure 1a is a layout of the 25 GeV/c ring tunnel. The inside dimensions of the tunnel are 7' wide by 7'6" high. The tunnel interfaces with the main ring with a 60 meter straight section. This straight section contains an enlarged experimental region 90' long by 19' wide by 16' high (see Figure 2a). There is another straight section of 60 meters opposite the main ring. This straight section will contain an access port 10' wide by 20' long. During machine construction it will be covered by a temporary structure to protect magnet installation from the weather. Afterwards it will have a small personnel and equipment entry. Most of it will be covered by shielding blocks. There are 2 additional short straight sections of 10 meters each.

The schedule for construction of the tunnel could be done in the following sequence:

0 week - Experiment Approved

2 weeks- Select A/E Firm

10 weeks- Bid Package Ready

3 weeks- Select Contractor

36 weeks- Construction

---

51 weeks- Beneficial Occupancy.

The construction of the experimental region and extraction area can be performed in a manner similar to the C0 construction. This can be done during a 4-week shutdown of the accelerator.

The cost of the tunnel is outlined in Table I. The total cost is estimated to be $1,089,000.00.

The schedule of the tunnel construction could be advanced by 2 months if Fermilab would invest $25,000 in the proposal prior to the Program Advisory Committee meeting. This would be used to have the A/E firm do most of the detailed drawings and cost estimate. This would not only advance the schedule, but would also provide Fermilab with an accurate estimate of the construction schedule and cost.

TABLE I

Small Storage Ring
Summary of Architectural Services Estimates of Costs
5th November 1975

1.	Inside dimensions of tunnel 7' wide, 7'6" high		
	Cost/linear foot =	$ 344	
	Contractor overhead, mark-up, etc. (21%)	76	
		$ 421	
	Subtotal at 2000'		$ 842 K
2.	Break into Main Ring	$ 9,000	
	Safety Hatches	$ 3,000	
	Lights	8,000	
	Sump Pump	6,000	
	Premium for fast construction of MR work	9,000	
		$ 35,000	
			$ 35 K
3.	Experimental Building at intersection region 90' long, 19' wide, 16' high.		
	Cost/linear foot =	$ 908	
	Subtotal		$ 82 K
4.	Miscellaneous		
	Access port 10' wide by 20' long	$ 10,000	
	Remove existing accelerator equipment	5,000	
	Electricity receptacles and lights	15,000	
	Miscellaneous	50,000	
		$ 80,000	
			$ 80 K
5.	A/E Services @ 5%		$ 50
6.	Add for contingencies		$ 100
	TOTAL		$1089

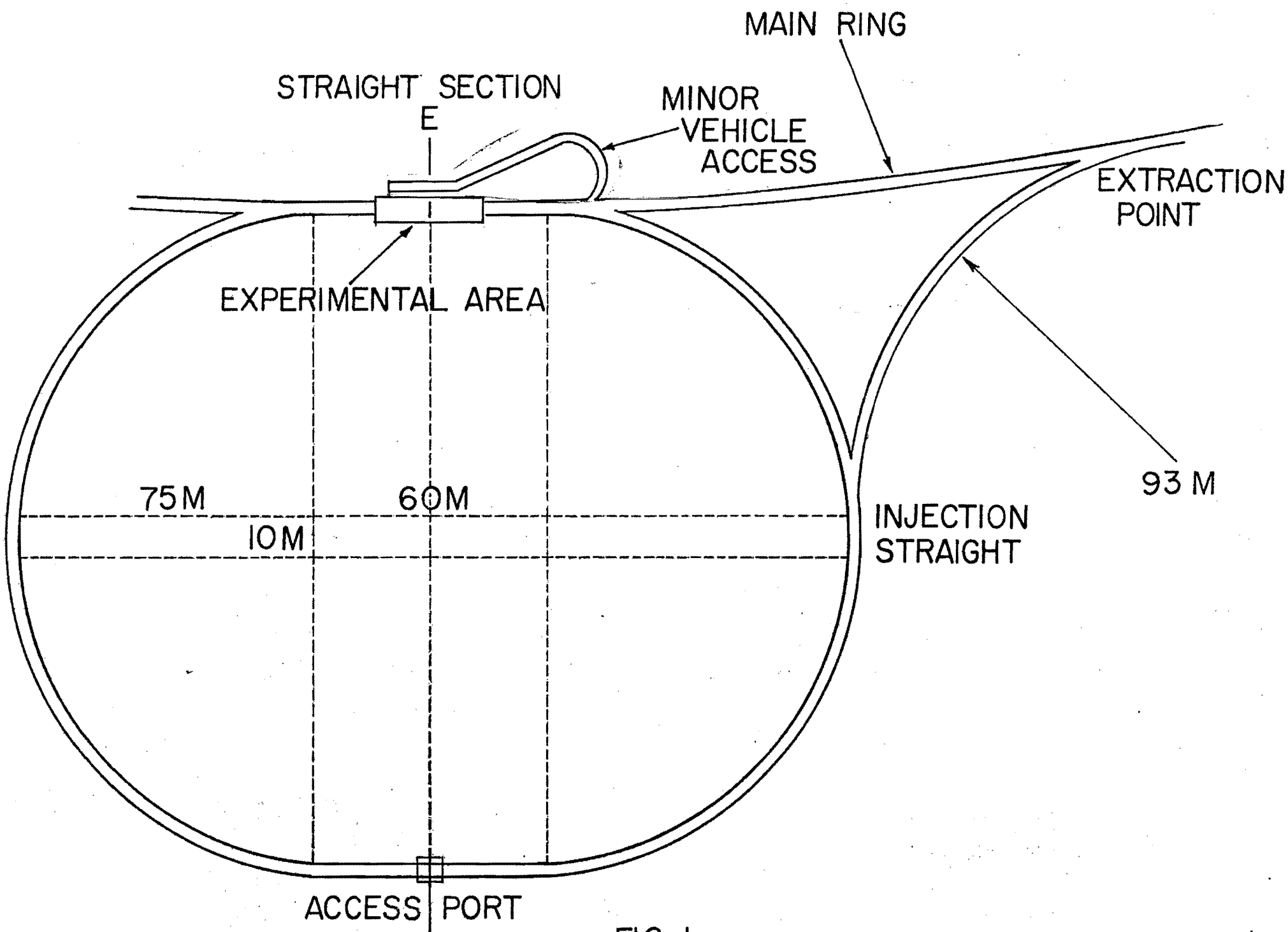
MAIN RING
STRAIGHT SECTION
E
MINOR
VEHICLE
ACCESS
EXTRACTION
POINT
EXPERIMENTAL AREA
93 M
75M
60M
10M
INJECTION
STRAIGHT
ACCESS PORT

FIG. 1a

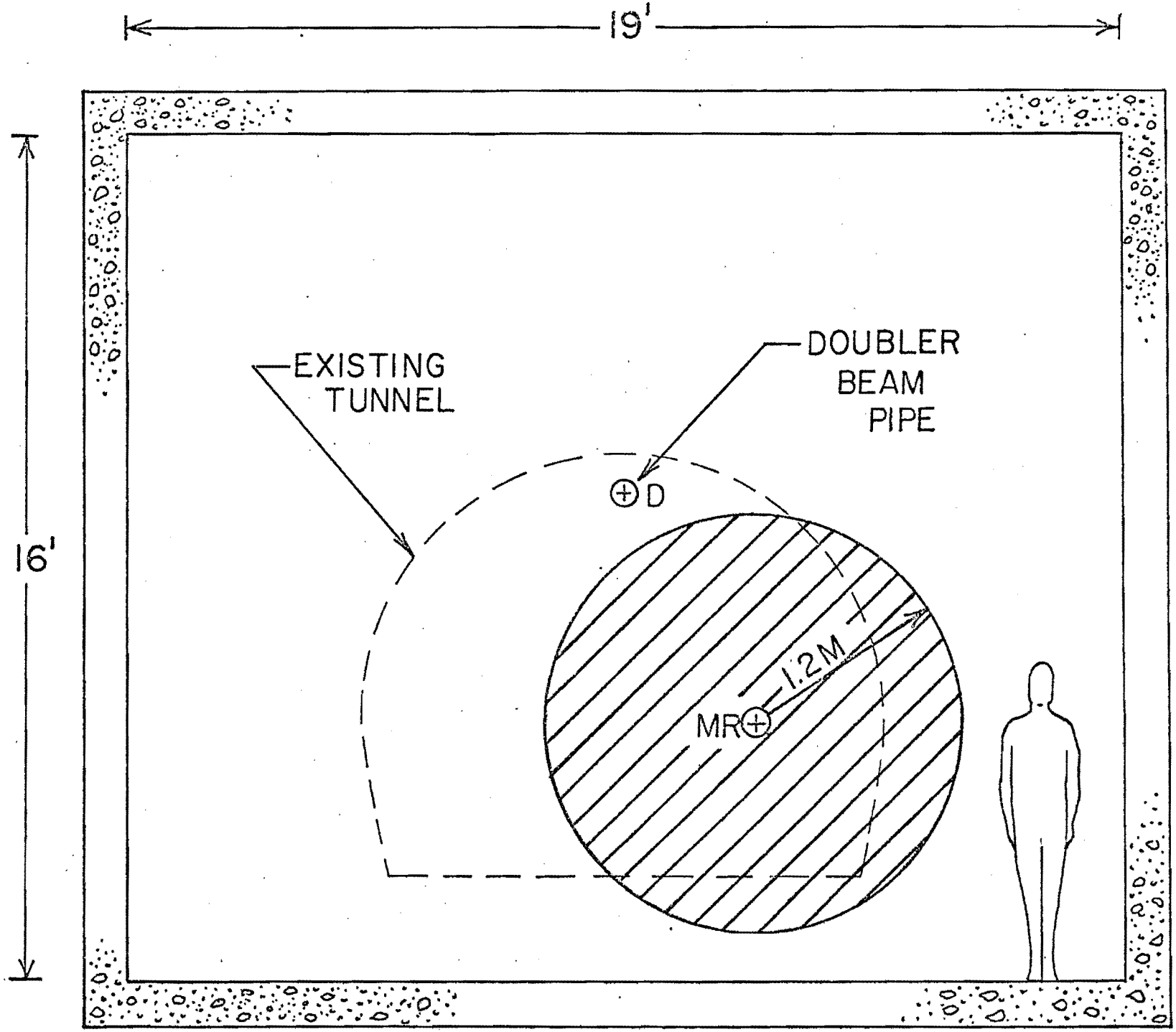

CROSS SECTION OF INTERFACING REGION

FIG. 2a

Appendix 2

Design of the Ring Magnets

The small storage ring magnets will be fabricated from stampings and have a simple pancake coil geometry. It is our intention to have the steel laminations made externally and stack them at FNAL. There are only 88 dipoles and we expect to reach a level of production of one per day without any trouble.

The coils are fabricated entirely in one plane and hence do not involve any complex winding procedures. Each pancake is inserted into a stacked core of laminations through the pole gap. It is then blocked up into position. Six individual but identical pancake coils are required for each dipole. Magnets can easily be disassembled and coils changed if required. The simplicity of design, allows ease of fabrication, allows us to do much of the work ourselves, and keeps the cost to a minimum.

The design of the quadrupoles follows the same procedure as for the dipoles.

We did originally consider using main ring or doubler magnets for the small ring. There are at least three reasons why these alternatives are not attractive. First, the maximum reasonable length of magnets for this small radius of curvature ring is about 10 feet. Secondly, the aperture of the magnets for the storage ring has to be quite large to allow the beam manipulation involved in the stacking procedure. Third, the field quality has to be high to successfully store beam for the periods of time required.

Schematic Cross Section Diagram

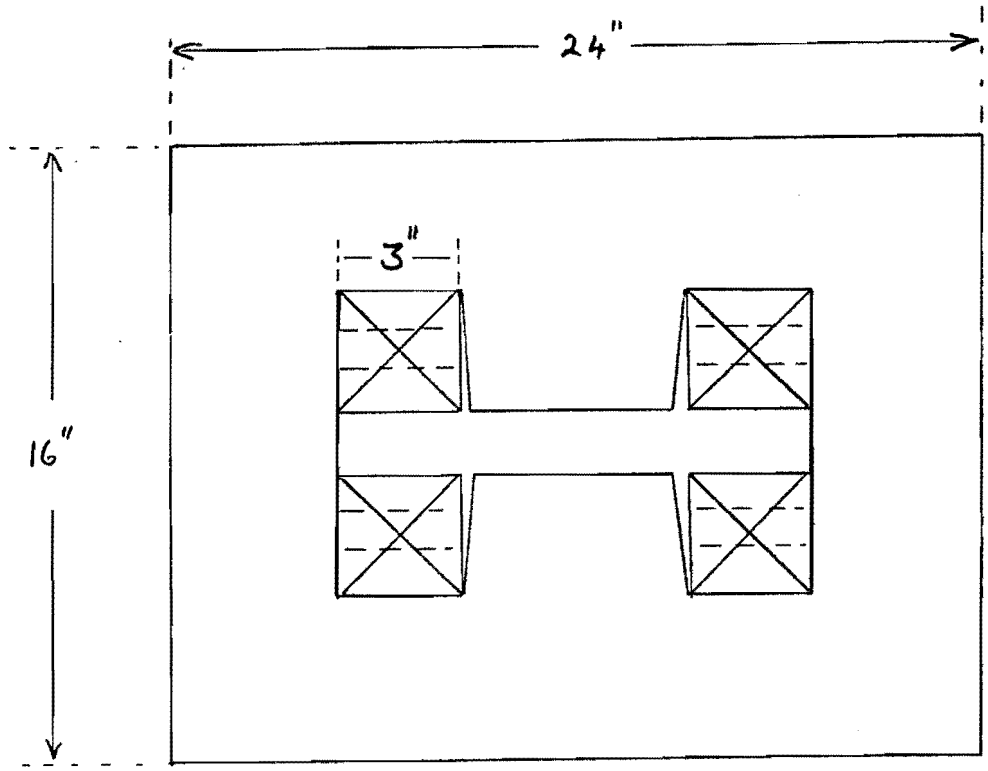

GAP	1 1/2" x 5"
LENGTH	10'
COPPER	3 x 3" x 2/3 Packing Factor/Turn
TURNS	40
18 kG CURRENT:	1375A
18 kG POWER :	64.13 kW
VOLTAGE DROP :	46.63 Volts
COPPER WEIGHT:	951#
COST $1/#	$951
LAMINATION WEIGHT BEFORE STAMPING	14299#
COST $0.18/#	$2573
FABRICATION COST	$3750
TOTAL COST	$7274

MAGNET SUMMARY

MAGNET	NUMBER	UNIT COST	TOTAL	D.C. POWER
SSR				
SSR DIPOLE	88	7274	640100	5.27 MW
SSR QUAD	48	4300	206400	.46 MW
SEXTUPOLE	32	1500	48000	.10 MW
			894500	6.03 MW
INSERTIONS				
DOUBLE DIPOLES	2	15000	30000	.15 MW
DIPOLES (1m)	4	2500	10000	.09 MW
MATCHING QUAD	20	3600	72000	0.18 MW
			112000	0.42 MW
INJECTION TRANSPORT				
SSR DIPOLE	16	7274	116400	1.00 MW
SSR QUAD	8	4300	34400	.08 MW
MATCHING QUAD	8	3600	28800	.07 MW
			179600	1.15 MW
INJECTION				
MAIN RING C	1	35000	35000	----
KICKER - MR	1	5000	5000	----
SEPTUM - MR	1	15000	15000	----
KICKER - SSR	1	5000	5000	----
SEPTUM - SSR	1	15000	15000	----
			75000	

TOTAL MAGNET COST $1,261,100

POWER SUPPLY SUMMARY - NOT INCLUDING 13.8kV CABLES

SSR DIPOLE SUPPLY		
4 - 1kV, 1500A Unregulated	$37000	148000
1 - 350V, 1500A Regulated	20000	20000
SSR QUADRUPOLE SUPPLIES		
2 - 350V, 1500A Regulated	20000	40000
SSR SEXTUPOLE		
1 - 200V, 500A Regulated	10000	10000
INSERTION DIPOLES		
2 - 350V, 500A Regulated	10000	20000
INSERTION QUADRUPOLES		
10 - 200V, 100A Regulated	20000	20000
INJECTION TRANSPORT		
2 - 350V, 1500A	20000	40000
PULSED KICKERS		
2 -	5000	10000
SEPTUM		
2 -	5000	10000
SS-DOUBLE DIPOLE		
1 - 200V, 50A Regulated	10000	10000
		$328000
BUS WORK		50000
		$378000

Appendix 3

High Vacuum System

1. Average Vacuum Required.

A decrease of luminosity with time will result from an increase of the cross-sectional area of the 25 GeV stored beam due to multiple scattering on the residual gas. If $\bar{r}(t)$ is the r.m.s. radius of the beam at time t, then

$$\bar{r}(t) = \sqrt{\bar{r}^2(0) + \bar{r}^2_{MS}(t)} \qquad (1)$$

If we design for a 20% change in L in 10 minutes, then

$$\bar{r}_{MS}(t = 600s) = \sqrt{1.2\ \bar{r}(0)^2 - \bar{r}^2(0)}$$
$$= 0.447\ \bar{r}(0)$$

For $\bar{r}_{MS}(t)$ we have

$$\bar{r}_{MS}(t) = \bar{\beta}\ Z\ r_e\ \frac{m_e c}{p} \sqrt{4\pi c(\ln \frac{\theta_c}{\theta_1})\ n_a\ t} \qquad (2)$$

$\bar{\beta}$ = average β function

Z = Z of residual gas

n_a = density of residual gas

$$\frac{\theta_c}{\theta_1} = \frac{\sqrt{2}\ y_{max}}{\bar{\beta}} \Big/ \alpha\ Z^{1/3} \quad \frac{m_e c}{p}\text{, with}$$

y_{max} = max. vertical aperture

For r_o = 1.28mm, $\bar{\beta}$ = 20m, Z = 7, and y_{max} = 13.5mm, we find

$$n_a = 2.91 \times 10^8\ \frac{\text{atoms}}{\text{cm}^3}$$

or

$$p = 4.1 \times 10^{-9} \text{ Torr.}$$

As a design goal we take an average pressure of 1×10^{-9} Torr for the 25 GeV storage ring; for the interaction region we need $\sim 10^{-10}$ Torr in order to limit beam-gas background.

2. Vacuum Chamber Design

The vacuum system will be all stainless steel (Type 304) with facility for in-place bake-out at 200°C. There will be flange joints only in the long straight sections, the semi-circular regions will consist of 3.75 m curved segments (Fig. 3A) welded together in place. Free space between magnets will be a 127 mm diameter pipe with one bellows to allow for alignment and expansion.

The cross section of the vacuum chamber in the bending magnets (see Fig. 3A) will be approximately rectangular with inside dimensions 102 mm x 27 mm. It will have a wall thickness of 2 mm; heaters ($\sim$ 6 w/cm) will be placed along both sides to allow for in-place bake-out. A 3 mm thick wrap of aluminum silicate paper will provide thermal insulation for bake-out.

3. Pumping System

The basic pumping scheme will be a modular one with one 20 ℓ/s sputter-ion pump every 3.75 m (see Fig. 3B). The interior surface area of a 3.75 m section is

$$A = 1.0 \times 10^{4} \text{ cm}^{2}.$$

The conductance, C, of this chamber is 4.6 ℓ/s for air at 22°C. Assuming a uniformly distributed gas load, the relation between average pressure and pumping speed, s, is

$$\bar{p} = \frac{Q_o}{s}\left(1 + \frac{s}{12C}\right) \qquad (3)$$

Hence for a $\bar{p} = 1 \times 10^{-9}$ Torr this system will handle a gas load, Q_o, of 1.47×10^{-8} Torr ℓ/s, corresponding to a thermal outgassing rate of 15×10^{-13} Torr-ℓ/s per cm^2 of surface. With careful chemical cleaning and baking under vacuum, outgassing rates of $\sim 2 \times 10^{-13}$ Torr ℓ/s cm^2 have been achieved with stainless steel. Furthermore, the prevailing residual gas at 10^{-9} Torr is H_2, for which the pumping speed of a 20 ℓ/s pump may be closer to 40 ℓ/s. For this geometry of vacuum chamber and pumps we estimate that the limit set by the pressure bump instability is $\eta I \lesssim 15A$.

The entire vacuum system will be separated into six sections by means of six fast-acting sector valves, two in each long straight and one in the middle of each half-circle. For initial pumpdown and bake-out there will be two 100 ℓ/s turbomolecular pumps per sector. Pumpdown from atmosphere to operating pressure will take approximately two days.

4. Cost Estimate.

1. Vacuum Chamber

a)	134 x 3.7 m chambers	$ 80 K
b)	2 x 60 m straights	15 K
c)	Gate valves	20 K
d)	140 x 20 ℓ/s ion pumps	56 K
e)	6 x 100 ℓ/s turbopumps	30 K
f)	Bakeable valves	6 K
g)	6 x 500 ℓ/s ion pumps	20 K

h)	Power supplies for ion pumps	$ 53 K
i)	Vacuum gauges and readouts	8 K
j)	Miscellaneous (pickup electrodes, clearing electrodes vacuum flanges)	30 K
k)	Bake-out equipment	35 K
		$ 353 K

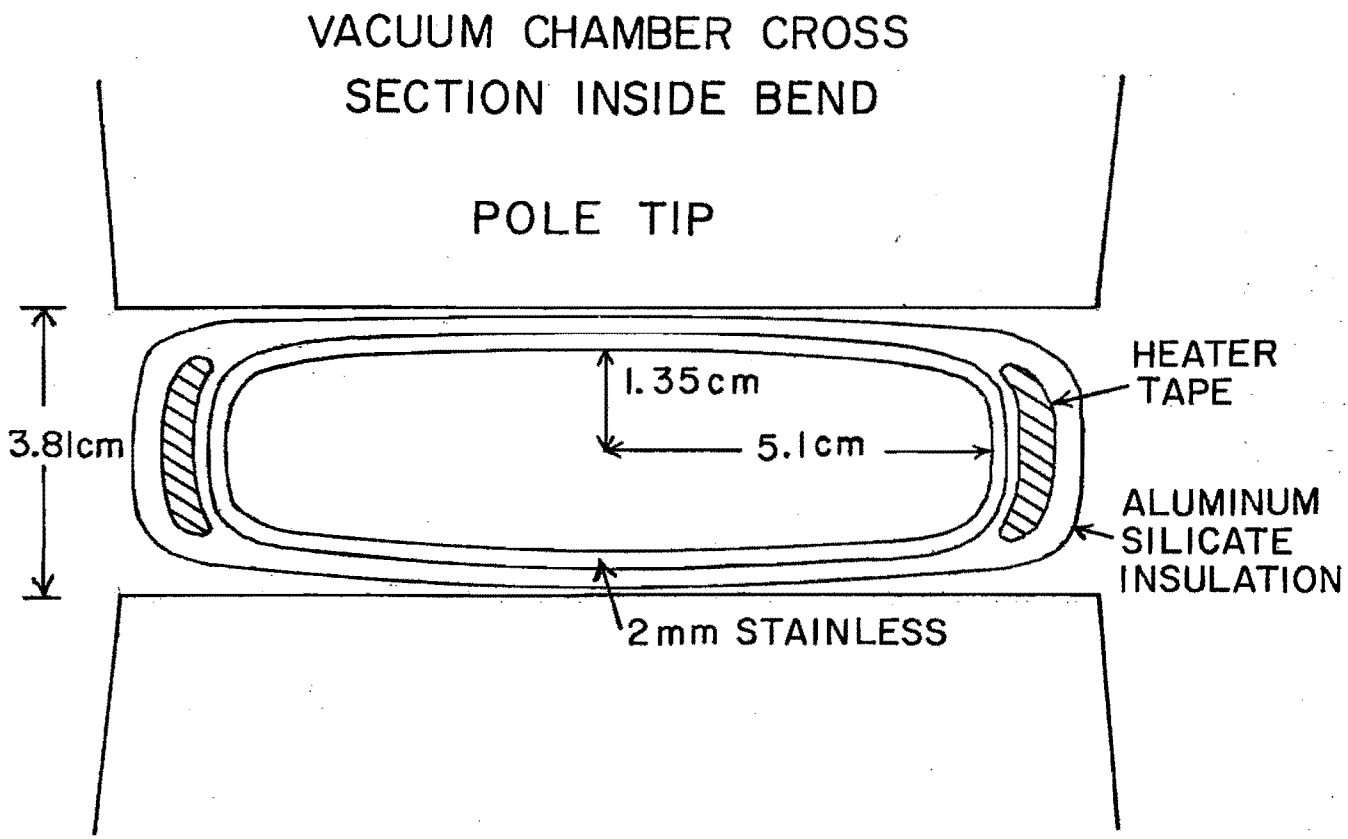

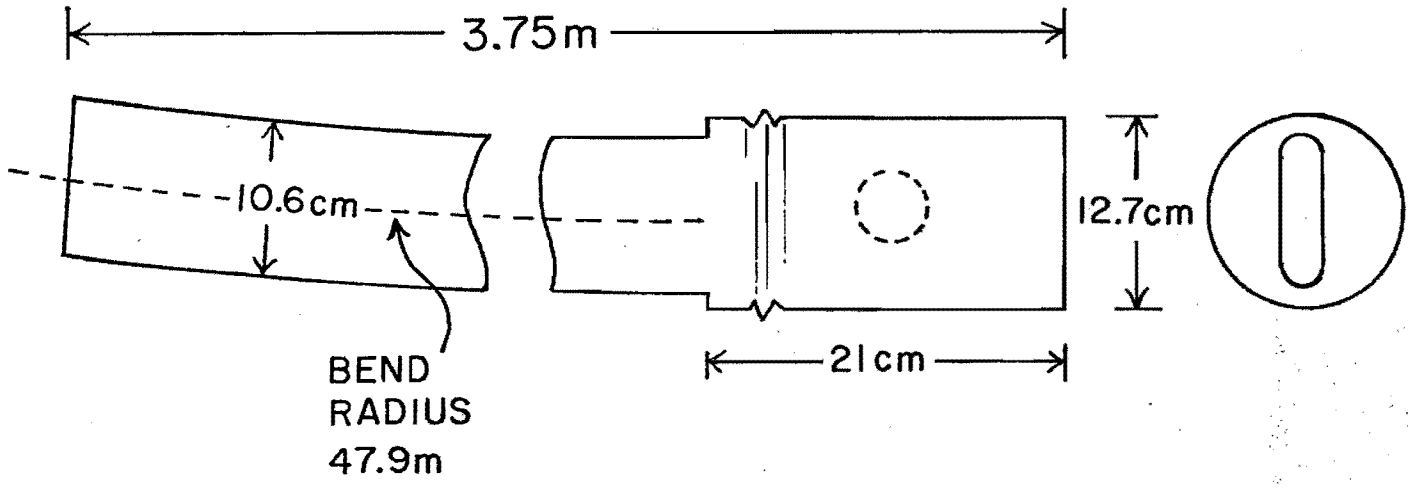

TOP VIEW OF BEND VACUUM CHAMBER

FIG. 3a

VACUUM LAYOUT OF HALF-CELL

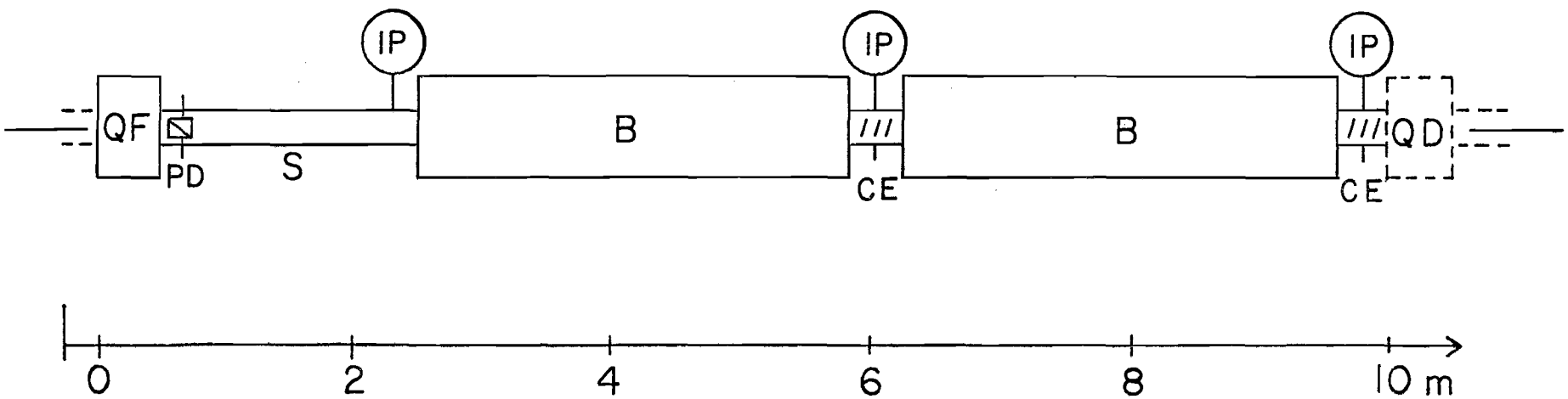

IP – 20ℓ/s ION PUMP

PD – POSITION DETECTOR

CE – CLEARING ELECTRODE

S – STRAIGHT SECTION

FIG. 3b

Appendix 4

Detection System Costs

1.	118	Steel slabs 10 cm x 2.4 m diameter at $1.4 K each	$ 165 K
2.		Coils plus power supplies	30 K
3.	59	Drift chamber modules construction at $2 K each	118 K
4.	59	Drift chamber module electronics at $30/wire and 88 wires/module	156 K
5.	20	Scintillation counters	100 K
		Total	$ 569 K

Appendix 5

Other Experimental Options for Achieving 200 GeV in the C.M.S.

1. We have considered other colliding beams involving the main ring and the energy doubler. For example, there is the possibility of colliding a 50 GeV beam in the main ring with a 1000 GeV beam in the doubler. A limit to the main ring energy of about 50 GeV is determined by the requirement of manipulating the beam to collide with the doubler beam within the 170 feet long straight distance. This approach would require shutting off the regular experimental program at FNAL for long periods of time. There is a large capital investment (∿ $100 M) in the external experimental areas and annual funds of ∿ $50 M are expended to exploit these facilities. To shut off these research areas would disrupt the experimental program at FNAL and be an inefficient use of the capital and operation funds. A variant of this scheme is to store the beam in the doubler and interact with the main ring beam during its acceleration between 25 and 50 GeV. Beyond 50 GeV the main ring beam would be switched back to its normal orbit. No disruption of the experimental program would occur in this approach. The disadvantages are that the duty cycle for beam beam interactions would be low and in addition the luminosity would be restricted due to inability to stack beam in the doubler. Furthermore, the switching of the main ring beam between the normal and colliding orbits could prove to be rather difficult. For these reasons neither of these approaches appear promising.

2. A second option considered, was the use of a dedicated low energy (50 GeV) beam located directly above the main ring and

intersecting it at two of the long straights. Although this approach minimizes interference with the research program it suffers from the disadvantages that the installation problems in the main ring tunnel are severe and couple strongly to the installation of the doubler in the same tunnel. For these reasons we discarded this option.

3. The scheme we propose has the following advantages:

a) Plant costs of the tunnel construction (∿ $1.0M) are a small part of the overall cost.

b) Installation and testing of components of the small ring can be done independently of main ring operation.

c) There is complete decoupling with the doubler project.

d) Operation of the small ring can proceed simultaneously with the rest of the experimental program.

e) Ability to stack the beam in the small ring gives an order of magnitude greater luminosity than other schemes.

f) The duty cycle for beam beam interactions is more than 50% and is superior to that in other schemes.

Appendix 6

Miscellaneous

1. R. F. System.

A single cavity at a peak voltage of 492 volts is adequate to manipulate and stack the stored beam. The system is quite simple and we estimate a cost of $30,000.

2. Additional Pumping Capacity in the Interaction Straight.

To reduce backgrounds in the interaction straight we anticipate the need to have a better vacuum ($\sim 10^{-10}$ torr) in the straight than in the rest of the small storage ring. An additional pumping capacity in the main ring for a 100' length upstream of the interaction straight will also be required to minimize backgrounds. We estimate the costs to be $30,000.

3. Sensors and Control Interface. $200,000

Total miscellaneous $300,000